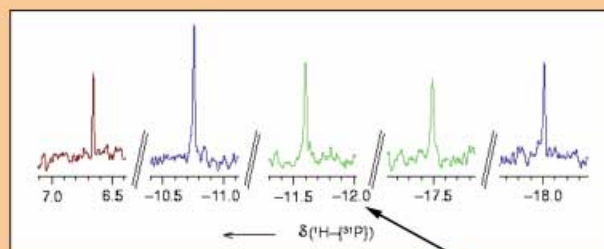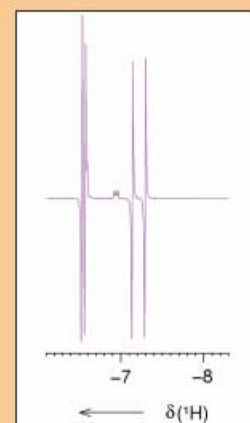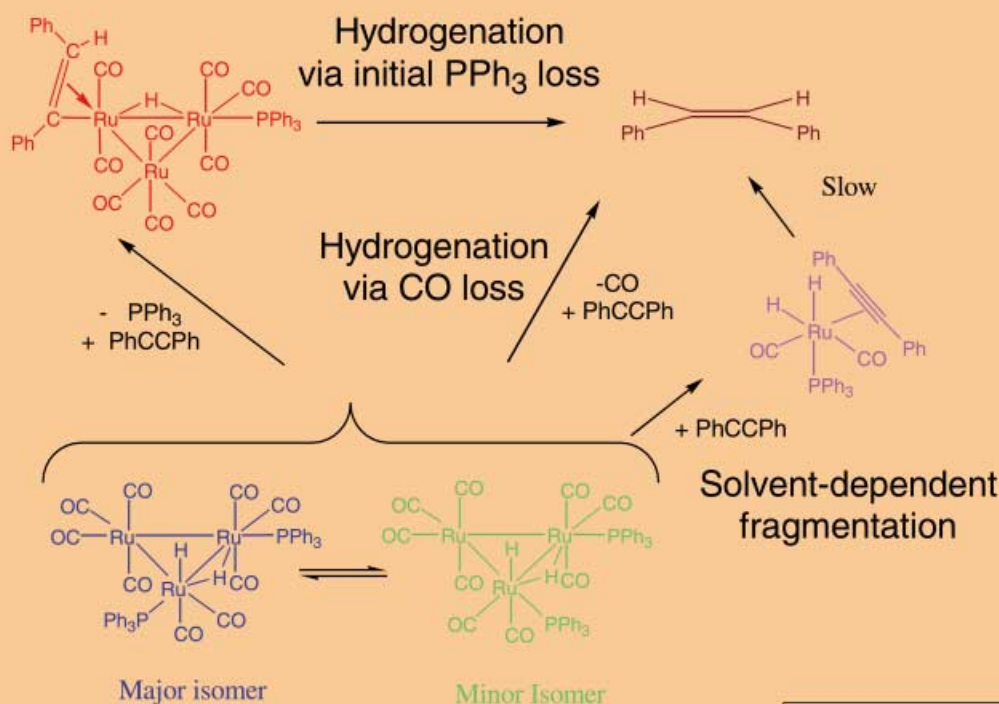# Direct evidence for cluster-based catalysis:

A parahydrogen story

Magnetisation transfer from this hydride site

Hydrogenation via initial PPh3 loss

Hydrogenation via CO loss

− PPh3 + PhCCPh

−CO + PhCCPh

Slow

+ PhCCPh

Solvent-dependent fragmentation

Major isomer

Minor Isomer

Styrene analogue
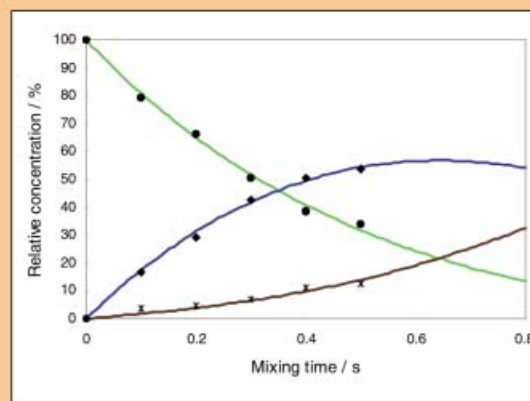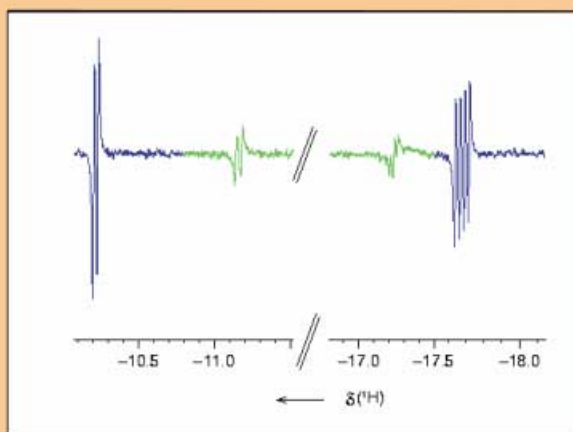
Kinetics of isomer exchange and hydrogenation for fast reacting minor isomer

For more information see the following pages.

Catalytic Hydrogenation by Triruthenium Clusters: A Mechanistic Study with Parahydrogen-Induced Polarization

Damir Blazina,[a] Simon B. Duckett,*[a] Paul J. Dyson,*[b] and Joost A. B. Lohman[c]

Abstract: The reactivity of the cluster family $[Ru_3(CO)_{12-x}(L)_x]$ (in which L = PMe_3, PMe_2Ph, PPh_3 and PCy_3, $x = 1-3$) towards hydrogen is described. When $x = 2$, three isomers of $[Ru_3(H)(\mu\text{-}H)(CO)_9(L)_2]$ are formed, which differ in the arrangement of their equatorial phosphines. Kinetic studies reveal the presence of intra- and inter-isomer exchange processes with activation parameters and solvent effects indicating the involvement of ruthenium-ruthenium bond heterolysis and CO loss, respectively. When $x = 3$, reaction with H_2 proceeds to form identical products to those found with $x = 2$, while when $x = 1$ a single isomer of $[Ru_3(H)(\mu\text{-}H)(CO)_{10}(L)]$ is formed. Species $[Ru_3(H)(\mu\text{-}H)(CO)_9(L)_2]$ have been shown to play a kinetically significant role in the hydrogenation of an alkyne substrate through initial CO loss, with rates of H_2 transfer being explicitly determined for each isomer. A less significant secondary reaction involving loss of L yields a detectable product that contains both a pendant vinyl unit and a bridging hydride ligand. Competing pathways that involve fragmentation to form $[Ru(H)_2(CO)_2(L)(alkyne)]$ are also observed and shown to be favoured by nonpolar solvents. Kinetic data reveal that catalysis based on $[Ru_3(CO)_{10}(PPh_3)_2]$ is the most efficient although $[Ru_3(H)(\mu\text{-}H)(CO)_9(PMe_3)_2]$ corresponds to the most active of the detected intermediates.

Keywords: cluster compounds · homogeneous catalysis · NMR spectroscopy · parahydrogen · ruthenium

Introduction

The chemical and physical properties of transition metal carbonyl clusters have been extensively studied over the last 40 years.[1] The primary thrust of much of this research was to produce homogeneous cluster catalysts that are able to replace heterogeneous catalysts used in important industrial processes.[2, 3] However, since organic substrates are able to adopt multicentre bonding modes with clusters, their reactivity might be expected to differ significantly from that found in their direct mononuclear analogues.[4] Recently, this has enabled organic transformations that are not possible by mononuclear homogeneous catalysts to be completed.[5]

One particularly well-studied group of clusters are the phosphine (L) derivatives of triruthenium dodecacarbonyl, $[Ru_3(CO)_{12-x}(L)_x]$ ($x = 1-3$),[6] which have been shown to catalyse numerous hydrogenation and hydroformylation reactions.[7, 8] The reactivity of these clusters towards hydrogen, as well as that of their iron and osmium analogues, has been extensively investigated.[9] It has been shown that the presence of the phosphine ligand markedly increases the catalytic activity of the precursor cluster.[7, 10] However, there is considerable debate over the exact nature and nuclearity of the active catalytic species involved in these reactions. Studies based on product yields and concentration effects indicate that fragmentation products are the active catalytic species in certain reactions.[11, 12] However, isotope labelling studies,[13] as well as the detection and isolation of hydride clusters that contain organic ligands[14] suggest that intact clusters can also act as catalysts. Since most studies of cluster catalysis have been indirect, these deductions usually rely on kinetic information and the analysis of the final metal-based product profiles. Hence, direct comparison of fragmentation and intact cluster catalysis, as well as rationalisation of the importance of the two pathways in catalysis, remain to be achieved.

With this in mind we set out to explore the precise mechanism of cluster catalysis by using a range of $[Ru_3(CO)_{12-x}(L)_x]$ clusters coupled with parahydrogen ($p\text{-}H_2$) NMR methods. This phenomenon, initially termed the

[a] Prof. Dr. S. B. Duckett, D. Blazina
Department of Chemistry, University of York
Heslington, York YO10 5DD (UK)
Fax: (+44)1904-432516
E-mail: sbd3@york.ac.uk

[b] Dr. P. J. Dyson
Institut de chimie moléculaire et biologique
Ecole Polytechnique féderale de Lausanne
EPFL-BCH, 1015 Lausanne (Switzerland)
E-mail: paul.dyson@epfl.ch

[c] J. A. B. Lohman
Bruker UK Limited, Banner Lane
Coventry CV4 9GH (UK)

PASADENA effect[15] and now usually referred to as para-hydrogen-induced polarisation (PHIP), has been reviewed.[16] Notable achievements in this area include the demonstration that PHIP effect enhances metal-hydride resonances directly, and those of scalar-coupled ^{31}P and ^{13}C heteronuclei by cross-relaxation[17] and cross-polarisation.[18] The development of selective excitation methods[19, 20] and the use of two-dimensional methods to facilitate the rapid indirect observation of insensitive heteronuclei nuclei have also made an impact.[21, 22] Other recent developments include studies of the adsorption of p-H$_2$ onto a solid surface[23] and studies with NMR shift reagents.[24] PHIP has also been employed in magnetic resonance imaging (MRI).[25]

Although applications of p-H$_2$ to cluster chemistry are much less common, some recent studies have been reported. Aime and Canet et al. have demonstrated that [Os$_3$-(μ-H)$_2$(CO)$_{10}$], a species with magnetically equivalent hydrides, can be studied.[26] The enhanced hydride signal observed here arises through the involvement of an intermediate with inequivalent hydrides. Interestingly, studies of [Ru$_3$(CO)$_{11}$(NCMe)] yielded an enhanced emission signal for molecular hydrogen; this indicates the reversible interaction of p-H$_2$ with the Ru$_3$ cluster containing inequivalent hydrides.[27] PHIP has recently been used to study triosmium μ_3-quinolyl trihydride clusters, whereby the observation of enhancement for all three hydride resonances has been attributed to the existence of fluxionality and cross-polarisation effects.[28] In these clusters, use of p-H$_2$ has led to the association of Os—Os bond breakage with the hydrogen addition step. Indirect evidence was also presented that H$_2$ can be transferred onto the quinolyl moiety, leading to its dissociation. A separate study of the hydrogenation of alkynes with [Os$_3$(μ-H)$_2$(CO)$_{10}$] led to the detection and character-isation of a range of vinyl hydride clusters by using p-H$_2$ and the transfer of polarised ^{1}H nuclei onto the bound organic substrates.[29]

Our group has previously used p-H$_2$ to detect new hydrogen addition products of [Ru$_3$(CO)$_{10}$(L)$_2$] (L = PMe$_2$Ph or PPh$_3$) and to follow their dynamic behaviour.[30] Here, we report on the use of phosphine-containing clusters [Ru$_3$(CO)$_{12-x}$(L)$_x$] ($x = 1-3$) in hydrogenation catalysis and present a detailed mechanistic study of their behaviour.

Results

All the complexes described in this paper are referred to according to the designation X-L, in which X indicates the compound number and L refers to the phosphine ligand. The structures of these species are shown in Figure 1. In the first section of the results and discussion we describe the hydrogen addition chemistry of [Ru$_3$(CO)$_{12-x}$(L)$_x$] ($x = 1-3$ and L = PCy$_3$, PMe$_3$, PMe$_2$Ph and PPh$_3$) before moving on to discuss roles of the corresponding products in catalytic hydrogenation.

Hydrogen addition to [Ru$_3$(CO)$_{10}$(PPh$_3$)$_2$] (1-PPh$_3$): When a solution of [Ru$_3$(CO)$_{10}$(PPh$_3$)$_2$] (1-PPh$_3$) in CDCl$_3$ is monitored by ^{1}H NMR spectroscopy in the presence of para-
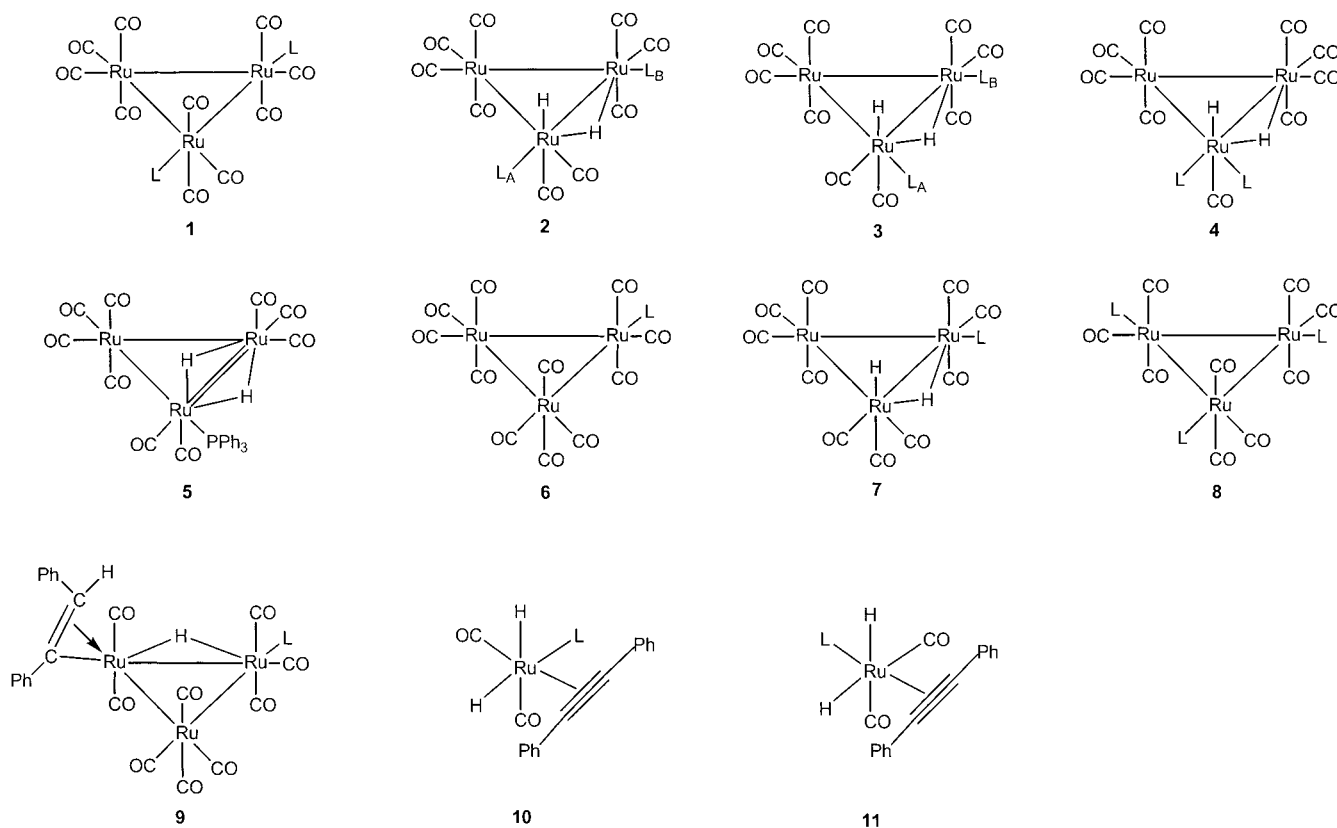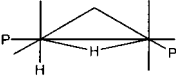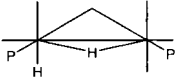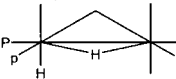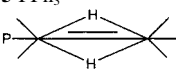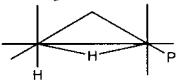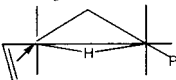

Figure 1. Compound structures (L = PMe$_2$Ph, PPh$_3$, PMe$_3$ or PCy$_3$). Compounds **1**, **6** and **8** reflect literature data, others identified here by NMR spectroscopy in solution.

hydrogen, three pairs of enhanced resonances and an emission signal were observed in the hydride region. The signals appearing at $\delta = -10.84$, -11.68 and -10.87 ppm arise from the terminal hydride ligands **2**-PPh$_3$-t, **3**-PPh$_3$-t and **4**-PPh$_3$-t of species **2**-PPh$_3$, **3**-PPh$_3$, **4**-PPh$_3$ respectively (t indicates a terminal position), while those at $\delta = -17.76$, -17.57 and -17.47 ppm arise from bridging hydrides **2**-PPh$_3$-b, **3**-PPh$_3$-b and **4**-PPh$_3$-b, respectively (b indicates a bridging position).[31, 32] The structures of **2**-PPh$_3$, **3**-PPh$_3$, **4**-PPh$_3$ and **5**-

PPh$_3$ are shown in Figure 1 and their NMR characteristics are listed in Table 1.

Characterisation of 2-PPh$_3$, 3-PPh$_3$, and 4-PPh$_3$, isomers of [Ru$_3$(H)(μ-H)(CO)$_9$(PPh$_3$)$_2$]: A full description of the characterisation of **2**-PPh$_3$, **3**-PPh$_3$, **4**-PPh$_3$ follows; it should, however, be noted that these species have been tentatively assigned previously.[33] For species **2**-PPh$_3$ and **3**-PPh$_3$, the terminal hydride signals both reveal couplings to single ^{31}P

Table 1. ^{1}H and ^{31}P NMR data at 296 K in CDCl$_3$ for hydrogen addition products with labelling according to Figure 1.[a]

Compound	δ ^{1}H	δ ^{31}P {^{1}H}	δ ^{13}C {^{1}H,^{31}P}
2-PPh$_3$	-10.84 (dd, $J_{PAH} = 11$ Hz, $J_{HH} = -4.5$ Hz; **2**-PPh$_3$-t),	44.60 (s; P$_A$), 31.25 (s; P$_B$)	198.0 (t, $J_{CC} = 8$ Hz), 200.2, 201.1,
	-17.76 (ddd, $J_{PBH} = 10$ Hz, $J_{PAH} = 20$ Hz, $J_{HH} = -4.5$ Hz; **2**-PPh$_3$-b)		202.3 (d, $J_{CC} = 8$ Hz), 204.3, 205.5
2-PMe$_2$Ph[b]	-11.10 (dd, $J_{PAH} = 13$ Hz, $J_{HH} = -4$ Hz; **2**-PMe$_2$Ph-t),	14.4 (s; P$_A$), -4.8 (s; P$_B$)	
	-18.15 (ddd, $J_{PBH} = 14$ Hz, $J_{PAH} = 18$ Hz, $J_{HH} = -4$ Hz; **2**-PMe$_2$Ph-b)		
2-PCy$_3$	-11.49 (dd, $J_{PAH} = 10$ Hz, $J_{HH} = -4$ Hz; **2**-PCy$_3$-t),	65.0 (s; P$_A$), 47.2 (s; P$_B$)	
	-18.38 (ddd, $J_{PBH} = 8$ Hz, $J_{PAH} = 20$ Hz, $J_{HH} = -4$ Hz; **2**-PCy$_3$-b)		
2-PMe$_3$	-11.65 (dd, $J_{PAH} = 14$ Hz, $J_{HH} = -4$ Hz; **2**-PMe$_3$-t),	7.23 (s; P$_A$), -12.30 (s; P$_B$)	
	-18.34 (ddd, $J_{PBH} = 13$ Hz, $J_{PAH} = 18$ Hz, $J_{HH} = -4$ Hz; **2**-PMe$_3$-b)		
3-PPh$_3$	-11.68 (dd, $J_{PAH} = 8$ Hz, $J_{HH} = -4.5$ Hz; **3**-PPh$_3$-t),	22.91 (s; P$_A$), 30.13 (s; P$_B$)	190.5, 198.1, 198.6, 199.9, 205.0
	-17.57 (ddd, $J_{PBH} = 9$ Hz, $J_{PAH} = 9$ Hz, $J_{HH} = -4.5$ Hz; **3**-PPh$_3$-b)		
4-PPh$_3$	-10.87 (td, $J_{PH} = 16$ Hz, $J_{HH} = -4.5$ Hz; **4**-PPh$_3$-t),	41.1 (s)	
	-17.47 (dd, $J_{PH} = 15$ Hz, $J_{HH} = -4.5$ Hz; **4**-PPh$_3$-b)		
4-PMe$_2$Ph[b]	-10.37 (td, $J_{PH} = 16.4$ Hz, $J_{HH} = -4.5$ Hz; **4**-PMe$_2$Ph-t),	-0.6 (s)	
	-18.61 (dd, $J_{PH} = 13$ Hz, $J_{HH} = -4.5$ Hz; **4**-PMe$_2$Ph-b)		
4-PMe$_3$	-10.98 (td, $J_{PH} = 16$ Hz, $J_{HH} = -3$ Hz; **4**-PMe$_3$-t),	-8.24 (s)	
	-18.88 (d, $J_{PH} = 14$ Hz, $J_{HH} = -3$ Hz; **4**-PMe$_3$-b)		
5-PPh$_3$	-14.35 (br s)	32.1 (s)	
5-PMe$_2$Ph[b]	-15.50 (br s)	-5.44 (s)	
5-PCy$_3$	-14.51 (br s)	54.38 (s)	
7-PPh$_3$[c]	-11.43 (s; **7**-PPh$_3$-t),	30.7 (s)	
	-18.34 (d, $J_{PH} = 10$ Hz; **7**-PPh$_3$-b)		
7-PCy$_3$[c]	-11.73 (s; **7**-PCy$_3$-t),	47.9 (s)	
	-18.81 (d, $J_{PH} = 7.5$ Hz; **7**-PCy$_3$-b)		
9-PPh$_3$	-13.32 (dd, $J_{PH} = 10$ Hz, $J_{HH} = -4.5$ Hz),	36.6 (s)	198.1, 200.5, 201.0, 203.8, 204.4
	7.50 (d, $J_{HH} = -4.5$ Hz)		
9-PMe$_2$Ph[c]	-13.74 (dd, $J_{PH} = 12$ Hz, $J_{HH} = -6$ Hz),	-5.03 (s)	
	7.47 (d, $J_{HH} = -6$ Hz)		
9-PCy$_3$	-13.94 (dd, $J_{PH} = 8$ Hz, $J_{HH} = -4.5$ Hz),	54.41 (s)	
	7.44 (d, $J_{HH} = -4.5$ Hz)		
10-PPh$_3$[d]	-6.54 (dd, $J_{PH} = 15$ Hz, $J_{HH} = -5.5$ Hz),	44.91 (s)	197.1 (d, $J_{CC} = 7$ Hz), 199.0 (d, $J_{CC} = 7$ Hz)
	-7.22 (dd, $J_{PH} = 62$ Hz, $J_{HH} = -5.5$ Hz)		
10-PMe$_2$Ph[d]	-7.02 (dd, $J_{PH} = 26$ Hz, $J_{HH} = -7$ Hz),	-1.66 (s)	
	-7.19 (dd, $J_{PH} = 75$ Hz, $J_{HH} = -7$ Hz)		
10-PCy$_3$[e]	-7.03 (dd, $J_{PH} = 14$ Hz, $J_{HH} = -5$ Hz),	54.22 (s)	
	-8.12 (dd, $J_{PH} = 66$ Hz, $J_{HH} = -5$ Hz)		
11-PCy$_3$[f]	-7.99 (2nd order, $J_{PH} = 14$ Hz, $J_{HH} = -5$ Hz)	54.93 (s)	194.9

[a] The remote atoms shown in thumbnail sketches contain Ru(CO)$_4$. [b] In [D$_8$]toluene. [c] At 233 K. [d] *cis,trans*-[Ru(H)$_2$(CO)$_2$(L)(styrene)], in C$_6$D$_6$. [e] *cis,trans*-[Ru(H)$_2$(CO)$_2$(L)(diphenylacetylene)], in C$_6$D$_6$. [f] *cis,cis*-[Ru(H)$_2$(CO)$_2$(L)(diphenylacetylene)], in C$_6$D$_6$.

nuclei, while the corresponding bridging hydride resonances show splittings due to two phosphorus nuclei. It can therefore be concluded that both these species contain [Ru(H)(PPh$_3$)-Ru(μ-H)(PPh$_3$)] arrangements. The $^2J_{HP}$ value for **2**-PPh$_3$-t is 11 Hz (coupling to a ^{31}P nucleus observed at $\delta = 44.60$ ppm), while the corresponding coupling for **3**-PPh$_3$-t is 8 Hz (^{31}P signal at $\delta = 22.91$ ppm). This indicates that the phosphine ligand on the {Ru(H)(PPh$_3$)} centre is *cis* to the terminal hydride in both species. In contrast, while the resonance for **2**-PPh$_3$-b contained $^2J_{HP}$ couplings of 20 and 10 Hz (^{31}P nuclei yield signals at $\delta = 44.60$ and δ 31.25 ppm respectively), that for **3**-PPh$_3$-b yielded identical $^2J_{HP}$ values of 9 Hz (^{31}P nuclei yield signals at $\delta = 22.91$ and 30.13 ppm). Based on these data it can be concluded that proton **2**-PPh$_3$-b is *trans* to the phosphine of the {Ru(PPh$_3$)H} centre, and *cis* to the other, while proton **3**-PPh$_3$-b is *cis* to both phosphines.[34] These arrangements are indicated in Figure 1.

For the third isomer, **4**-PPh$_3$, both the terminal and bridging hydride resonances appear as triplets of anti-phase doublets due to equal coupling to two ^{31}P nuclei. These results place the two phosphines of **4**-PPh$_3$ on the same ruthenium centre as the terminal hydride ligand and should to result in the observation of two ^{31}P signals for the expected inequivalent equatorial phosphines ligands. However, the observation of equivalent H-P splittings is further backed up by the observation of a single ^{31}P signal at $\delta = 41.10$. This requires the two phosphine ligands in **4**-PPh$_3$ to rapidly exchange positions at 296 K. Such a situation has been suggested previously.[30]

In order to monitor the carbonyl environments of these complexes, 100 % ^{13}C-enriched samples of **1**-PPh$_3$ were prepared. These were examined in the presence of an excess of diphenylacetylene in order to increase signal intensity (see later). Typical spectra illustrating the ^{13}C investigation are shown in Figure 2. Since each of the low-field hydride resonances now possess an additional ^{1}H–^{13}C coupling of approximately 16 Hz (obtained by simulation), a *trans* ^{1}H-Ru-^{13}CO arrangement is indicated for this ligand.[35] A series of ^{1}H-^{13}C HMQC spectra were recorded to determine the chemical shifts of the associated carbon signals for the carbonyl groups in products **2**-PPh$_3$ and **3**-PPh$_3$. These spectra revealed the presence of six different ^{13}CO resonances in **2**-PPh$_3$, and five ^{13}CO resonances in **3**-PPh$_3$, which arise from the nine CO ligands contained in these products. In all cases, the ^{13}C chemical shifts were indicative of terminal carbonyl groups[36] and no signals were seen that could be attributed to bridging carbonyl ligands.

These features deserve more comment. In particular, it should be noted that in the case of **2**-PPh$_3$, connections from the signal due to proton **2**-PPh$_3$-t appear to two carbonyl resonances at $\delta = 200.2$ and 201.1 ppm. Furthermore, the broadness of these resonances suggests that rapid carbonyl ligand exchange is occurring. This result is not surprising considering the widely reported carbonyl fluxionality of [M$_3$(CO)$_{12}$] clusters and their derivatives, where M = Fe,[37] Ru[38] or Os.[39] Analogous behaviour has also been reported for the carbonyl ligands of [Os$_3$(μ-H)$_2$(CO)$_{10}$] and its derivatives.[40] Previous reports indicate that the chemical shifts of equatorial carbonyl signals appear at lower values than axial ones.[36] It can therefore be concluded that the resonance at
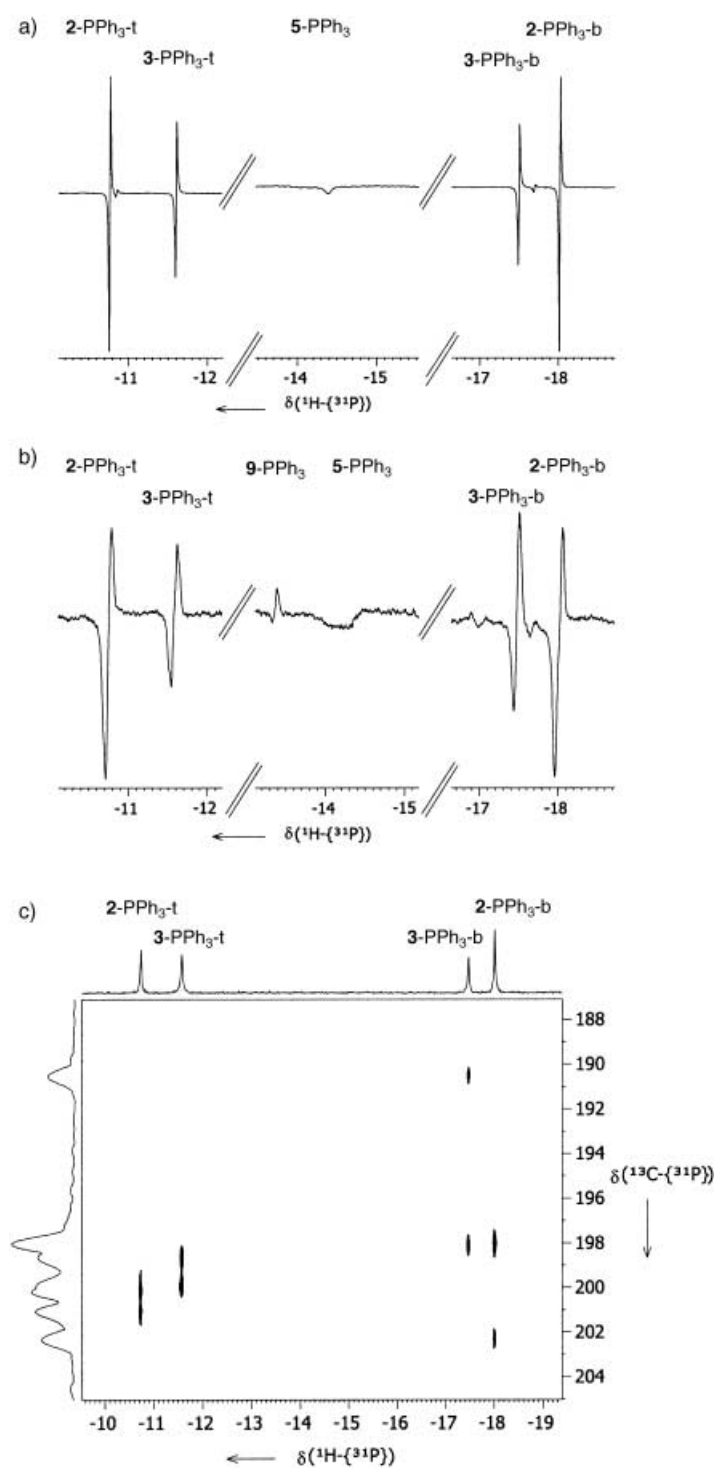
Figure 2. *p*-H$_2$-enhanced NMR spectra of **1**-PPh$_3$ obtained with an initial 100-fold excess of diphenylacetylene in CDCl$_3$ at 307 K recorded after 3 minutes of reaction: a) ^{1}H-{^{31}P} spectrum, b) ^{1}H-{^{31}P} spectrum of a ^{13}C labelled sample revealing enhanced peak separations due to ^{1}H–^{13}C couplings and c) selected cross-peaks (absolute value display) and projections showing hydride and carbonyl chemical shift correlations in a typical ^{1}H-^{13}C-{^{31}P} HMQC spectrum.

$\delta = 200.2$ ppm corresponds to a carbonyl ligand in the equatorial plane that is *cis* to the bridging hydride, while that at $\delta = 201.1$ is assigned to an axial carbonyl group. We have thus conclusively identified all the constituents of an {Ru(H)-

(CO)$_2$(PPh$_3$)} group. In a similar way, connections from proton **2**-PPh$_3$-t to signals at $\delta = 198.0$ and 202.3 ppm were observed. These correspond to signals from equatorial and axial carbonyl ligands of the {Ru(μ-H)(PPh$_3$)(CO)$_3$} centre.

Interestingly, when longer mixing times are used in the ^{1}H-^{13}C-{^{31}P} HMQC experiment, both the hydride resonances show cross-peaks to all four of these carbonyl resonances and to two further signals at $\delta = 204.3$ and 205.5 ppm. These last two connections are picked up as a result of ligand exchange, which facilitates magnetisation transfer onto the carbonyl ligands sites on the remote ruthenium centre. This supposition is supported by the fact that the corresponding carbonyl resonances of **1**-PPh$_3$ are observed at $\delta = 206.5$ ppm (br s) under these conditions. We propose the signal at $\delta = 205.5$ ppm is due to two equivalent axial carbonyls, while the signal at $\delta = 204.3$ ppm corresponds to the two apparently equivalent equatorial carbonyls.[30, 33, 38] By using this approach, the complete characterisation of **2**-PPh$_3$ was facilitated; the structure of **3**-PPh$_3$ was assigned in a similar way. It should be noted that although the analogous complex [Ru$_3$-(μ-H)$_2$(CO)$_{11}$] adopts a structure with a bridging carbonyl ligand,[27] we see no evidence for such an isomer in these substituted systems. It is not unreasonable to suggest that the steric bulk of the phosphines might lengthen the metal–metal bonds, thus favouring terminal carbonyls.

The remaining hydride signal at $\delta = -14.35$ ppm corresponds to the fourth product **5**-PPh$_3$. It should be noted that this resonance was extremely broad (ca. 150 Hz) and did not possess any resolvable fine structure between 307 and 233 K. Since the hydride resonance is observed as an emission signal, this species must be formed indirectly, via an intermediate with inequivalent hydride ligands.[27] In addition, since the associated resonance is very broad we conclude that this species is highly fluxional. Unfortunately, ^{13}CO labelling did not provide any further information for the characterisation of **4**-PPh$_3$ and **5**-PPh$_3$. The identity of **5**-PPh$_3$ will be discussed again later, although its proposed structure can be seen now in Figure 1.

It would be sensible at this stage to comment on the relative amounts of **2**-PPh$_3$:**3**-PPh$_3$:**4**-PPh$_3$ present in solution. In the associated ^{1}H NMR spectra, the ratio of the PHIP enhanced hydride resonances of **2**-PPh$_3$:**3**-PPh$_3$:**4**-PPh$_3$ corresponded to 58:9:1 at 296 K. Normally this integral data would equate directly with their relative ratios. However, in this case, this deduction is only valid if the magnitudes of the hydride signal enhancements are equal. We believe this to be the case, since similar peak ratios are observed at 244 K at which these species become visible by using normal methods after an overnight data acquisition of 10000 scans. This information confirms that **2**-PPh$_3$ is more stable than **3**-PPh$_3$, which in turn is more stable than **4**-PPh$_3$.

Effect of varying the phosphine on the product distribution: We have previously described how the two related hydrogen addition products **2**-PMe$_2$Ph and **4**-PMe$_2$Ph are observed when p-H$_2$ is added to the analogous cluster [Ru$_3$(CO)$_{10}$-(PMe$_2$Ph)$_2$].[30] Key NMR parameters for these species are presented in Table 1 for comparison purposes. We note that the relative PHIP enhanced hydride signal intensities for **2**-PMe$_2$Ph and **4**-PMe$_2$Ph suggest a 2.5:1 distribution in CDCl$_3$

at 296 K; no signals for species analogous to **3**-PPh$_3$ or **5**-PPh$_3$ were observed.

When the reaction of [Ru$_3$(CO)$_{10}$(PMe$_3$)$_2$] (**1**-PMe$_3$) with p-H$_2$ was monitored by NMR spectroscopy, the corresponding ^{1}H NMR spectrum contained enhanced hydride signals at $\delta = -10.98, -11.65, -18.34$ and -18.88 ppm. The identities of the corresponding products were confirmed as **2**-PMe$_3$ and **4**-PMe$_3$ in a similar manner to that described earlier for **1**-PPh$_3$. The two products exist in a ratio of 1.1:1. NMR data for these species can be found in Table 1. Once again, no signals for structures corresponding to **3**-PMe$_3$ or **5**-PMe$_3$ were observed.

The final bis-substituted cluster to be examined in this study was [Ru$_3$(CO)$_{10}$(PCy$_3$)$_2$] (**1**-PCy$_3$). When a solution of **1**-PCy$_3$ in CDCl$_3$ under an atmosphere of p-H$_2$ was monitored by ^{1}H NMR spectroscopy at 296 K, three hydride resonances are observed at $\delta = -11.49, -14.51$ and -18.38 ppm (see Table 1). COSY spectra confirmed the anti-phase doublet of doublets at $\delta = -11.49$ ppm coupled to the anti-phase doublet of doublets of doublets at $\delta = -18.38$ ppm, with similar coupling values to those already described for **2**-PPh$_3$; this indicates that these two signals arise from **2**-PCy$_3$. The remaining resonance at $\delta = -14.51$ ppm appeared as an emission signal at short reaction times, and is suggested to be due to **5**-PCy$_3$ with an analogous structure to **5**-PPh$_3$ (see later).[27] No signals for species that would correspond to **3**-PCy$_3$ or **4**-PCy$_3$ were observed in this reaction.

These observations indicate that the relative abundance of the various H$_2$ addition products formed in these reactions depends on the identity of the phosphine. In all cases, the dominant form of the isomer detected in solution corresponds to isomer **2**. In **2**, the two phosphines are placed further apart than in either **3** or **4** and steric interactions would be minimised. However, it should be noted that a further isomer is possible in which the phosphines are arranged mutually *trans* to the metal–metal bond. Such an arrangement has been discovered in the solid state for bis-substituted clusters of the type [Ru$_3$(CO)$_{10}$(L)$_2$], in which L = phosphine.[41] We therefore conclude that the electronic properties of the phosphine must play a role in controlling the final product distribution. This is clearly supported by the fact that isomer **3** is observed only for the least basic phosphine PPh$_3$, and not for PMe$_3$ or PCy$_3$.[42] In isomer **4**, both phosphines are located on the ruthenium centre that houses the terminal hydride ligand. Clearly, this species must also be formed for electronic reasons, but the steric strain expected from placing two phosphines on the same ruthenium centre is consistent with the abundance of **4** decreasing from $33 \rightarrow 26 \rightarrow 2 \rightarrow 0\%$ for L = PMe$_3$, PMe$_2$Ph, PPh$_3$ and PCy$_3$ respectively.

It should be noted that the highly unsaturated cluster [Ru$_3$H$_2$(CO)$_6$(PCy$_3$)$_3$] has been reported in the literature,[43] but no analogous species have been observed here. However, this is not surprising since the synthesis of the unsaturated species required significantly different reaction conditions to those employed in this study.

Observation and characterisation of the mono-substituted hydrogen addition products [Ru$_3$(H)(μ-H)(CO)$_{10}$(L)]: ^{1}H NMR observation of the cluster [Ru$_3$(CO)$_{11}$(PPh$_3$)] (**6**-PPh$_3$) in the presence of p-H$_2$ in CDCl$_3$ at 296 K led to

the detection of a new species **7**-PPh$_3$ as evidenced by two broad hydride resonances at $\delta = -11.43$ and -18.34 ppm. At 233 K, the terminal hydride signal at $\delta = -11.43$ ppm was sufficiently sharp to enable the confirmation that there was no ^{31}P coupling, while the bridging hydride signal at $\delta = -18.34$ ppm showed a 10 Hz coupling indicative of the presence of a *cis* phosphine. This data confirms that **7**-PPh$_3$ contains a {Ru(H)(μ-H)Ru(PPh$_3$)} arrangement. The corresponding structure of **7**-PPh$_3$ is shown in Figure 1 and the NMR characteristics of this species are listed in Table 1.

While the corresponding PCy$_3$-substituted cluster **6**-PCy$_3$ yielded signals characteristic of **7**-PCy$_3$ at $\delta = -11.73$ and -18.81 ppm (see Table 1 and Figure 1), the PMe$_2$Ph analogue **6**-PMe$_2$Ph yielded only a very broad (150 Hz) emission signal at $\delta = -15.50$ ppm in [D$_8$]toluene at 296 K, which was not observable below 285 K. The characteristics of this resonance indicate that there is very rapid transfer of magnetisation into this species from an unobserved dihydride complex with inequivalent hydrides.[27] On the basis of the hydride chemical shift, this complex is suggested to have the structure **5**-PMe$_2$Ph.[34]

Characterisation of the products formed by hydrogen addition to [Ru$_3$(CO)$_9$(L)$_3$]: On *p*-H$_2$ addition to [Ru$_3$(CO)$_9$(P-Me$_2$Ph)$_3$] (**8**-PMe$_2$Ph) and [Ru$_3$(CO)$_9$(PPh$_3$)$_3$] (**8**-PPh$_3$), products with identical NMR characteristics to those obtained from the bis-substituted clusters **1**-PMe$_2$Ph and **1**-PPh$_3$ were observed (same chemical shift, signal intensity, and ^{1}H–^{31}P couplings). There are two possible explanations for this, either the third metal centre does not affect the hydride resonances in any way, or the hydrogen addition product is formed through PPh$_3$ loss and subsequent rearrangement. The latter hypothesis has been proposed previously.[7] Since the hydride signal intensities for these species are much lower than those obtained when **1** is the precursor, we conclude that the loss of a phosphine ligand from **8**-PPh$_3$ is much less efficient than loss of CO from **1**-PPh$_3$. This observation agrees with the lower catalytic activity of such tris-substituted precursors.[7]

In the preceding sections we have described how *p*-H$_2$ enables the detection of a number of new clusters containing hydride ligands that might be expected to play a role in catalysis. We now describe how studies of the reactions of the same precursors with *p*-H$_2$ and suitable hydrogenation substrates support this view.

Catalytic hydrogenation of diphenylacetylene by 2-PPh$_3$ and 3-PPh$_3$: When a sample of **1**-PPh$_3$ was examined in CDCl$_3$ at 296 K with *p*-H$_2$ and in the presence of a 100-fold excess of diphenylacetylene, the ^{1}H NMR spectrum shown in Figure 3 was obtained. Initially, enhanced hydride resonances matching those described for **2**-PPh$_3$, **3**-PPh$_3$, **4**-PPh$_3$ and **5**-PPh$_3$ are present with similar intensities to those observed in the absence of substrate. However, the signal intensities associated with **2**-PPh$_3$ and **3**-PPh$_3$ rapidly increase in size (by a factor of 5 for **2**-PPh$_3$ and a factor of 32 for **3**-PPh$_3$) until after 30 s they have comparable intensities. Hydrogenation is evident in these spectra from the PHIP-enhanced signals for PhH^{13}C=^{12}CHPh,[44] a result not entirely surprising in view of previous discoveries of highly reactive and selective cluster
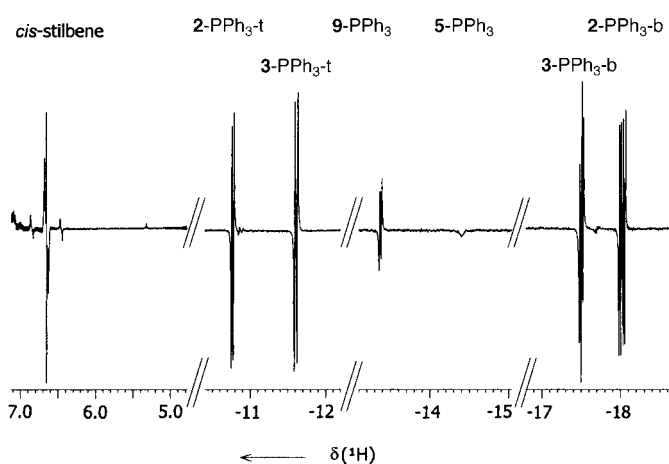

Figure 3. Key regions of a 256 scan ^{1}H NMR spectrum obtained from a sample of **1**-PPh$_3$ with *p*-H$_2$ in CDCl$_3$ in the presence of a 100-fold excess of diphenylacetylene recorded immediately after sample introduction into the spectrometer.

catalysts for the hydrogenation of diphenylacetylene.[45] The presence of hydrogenation makes it possible to conclude that the gain in hydride signal intensity arises from the increase in the rate of hydrogen cycling that results from sacrificial hydrogenation.[46] However, since the intensities of the hydride signals associated with **4**-PPh$_3$ show only minor enhancement over those seen without substrate, it can be deduced, qualitatively, that this species is a poorer hydrogenation catalyst than the other two.

Surprisingly, a new signal due to a bridging hydride that coupled to a single phosphorus centre was also observed in these spectra at $\delta = -13.32$ ppm ($J_{HP} = 10$ Hz, to a *cis* ^{31}P resonance located at $\delta = 36.6$ ppm by HMQC). Since the associated coupling partner appears at $\delta = 7.50$ ppm, the new species, **9**-PPh$_3$, contains a pendant μ-η^2 vinyl unit and a bridging hydride (see Table 1 for NMR data).[47] When the mono-substituted cluster **6**-PPh$_3$ was used as the precursor, the signals for **9**-PPh$_3$ were substantially larger, and hence this product can be deduced to contain a single phosphine.

By using a sample of **1**-PPh$_3$-^{13}C, full NMR characterisation of **9**-PPh$_3$ was attempted. When a short mixing delay was used in the ^{1}H-^{13}C-{^{31}P} HMQC experiment, the ^{13}C resonance for the carbonyl ligand *trans* to the bridging hydride was detected at $\delta = 198.1$ ppm. Upon changing to a longer evolution time, four other carbonyl resonances were detected at $\delta = 200.5$, 201.0, 203.8 and 204.4 ppm. Rapid carbonyl exchange prevented the observation of any ^{13}C–^{13}C couplings due to line-broadening effects.[37]–[40] The two resonances at $\delta = 203.8$ and 204.4 ppm can, however, be assigned to the equatorial and axial carbonyl carbons on the remote ruthenium centre, since their chemical shifts are very similar to those described earlier for **2**-PPh$_3$ and **3**-PPh$_3$. The remaining three resonances indicate the presence of only three distinct carbonyl environments on the two remaining ruthenium centres. In view of the fact that **9**-PPh$_3$ is formed by phosphine loss from **2**-PPh$_3$ and **3**-PPh$_3$ and by CO loss from **7**-PPh$_3$, five carbonyl ligands are expected to be attached to these centres. This requires **9**-PPh$_3$ to contain two pairs of axial CO ligands and one carbonyl in the equatorial plane. The vinyl ligand must therefore be

located in an equatorial μ-η^2 arrangement, as shown in Figure 1 (see also the Supporting Information).[48]

Interestingly, the intensities and relative ratios of the hydride signals that are observed in these experiments show a substantial variation with solvent (Figure 4). In order to rationalise these results in a quantitative fashion (see Supporting Information), NMR tubes containing 1-PPh₃ and a 100-fold excess of diphenylacetylene were charged with 3 atmospheres of hydrogen at 296 K and then rapidly introduced into the NMR probe. Subsequently, an exploration of both the dynamic behaviour of the hydride ligands in 2-PPh₃ and 3-PPh₃ and their transfer into the substrate was undertaken by using quantitative exchange spectroscopy (EXSY) measurements.[22, 30, 46] EXSY spectra were recorded for a variety of mixing times, temperatures and solvents, and the resultant data analysed according to the procedure outlined in the Supporting Information. It should be noted that when the H₂ available in solution is depleted (ca. 15 min), all the hydride resonances disappear from the corresponding ¹H NMR spectra and hydrogenation stops.

Quantitative analysis of the hydride exchange pathways in 2-PPh₃ and 3-PPh₃: A typical high-resolution 2D EXSY spectrum recorded over the hydride region for a sample of 1-PPh₃ in CDCl₃ in the presence of p-H₂ and diphenylacetylene is shown in Figure 5. The observation of positive exchange cross-peaks between *all* the hydride resonances of 2-PPh₃ and 3-PPh₃ indicates that *all* the hydride ligands interchange within the four available positions. Analysis of the NMR data for 301 K (see Supporting Information) produced the data illustrated in Figure 6. These exchange processes were subsequently explored in CDCl₃, [D₈]THF and [D₈]toluene over the temperature range 284–312 K. The associated rate constants and activation parameters are listed in Tables 2 and 3, respectively.

It should be noted that reductive elimination of hydrogen from 2-PPh₃ and 3-PPh₃ is not observed on this timescale and that although exchange of these hydrides into positions associated with 4-PPh₃ was observed, this route was could not be reliably quantified due to the low intensity of the corresponding cross-peaks.

Quantitative investigation of hydrogenation of diphenylacetylene by 2-PPh₃ and 3-PPh₃: When these ¹H NMR spectra are first recorded, enhanced signals for the product *cis*-stilbene are evident, indicating that hydrogenation is rapid (see Figure 3).[44] When this process is followed by 1D EXSY methods (in which the kinetic fate of a single hydride ligand can be monitored), depending on the conditions direct transfer of magnetisation from the hydride ligands of 3-PPh₃ into 2-PPh₃, 5-PPh₃, 9-PPh₃ and *cis*-stilbene could be observed, as shown in Figure 7a. When 2-PPh₃ was selected, the corresponding exchange pathways were again observed, although no exchange into 9-PPh₃ was detected. When the hydride 9-PPh₃-b was selected, transfer into the hydrogenation product was again observed.

The observed rate constants (k_{obs}) for alkene formation from 2-PPh₃, 3-PPh₃ and 9-PPh₃ were determined from these data in a variety of solvents at early reaction times where the
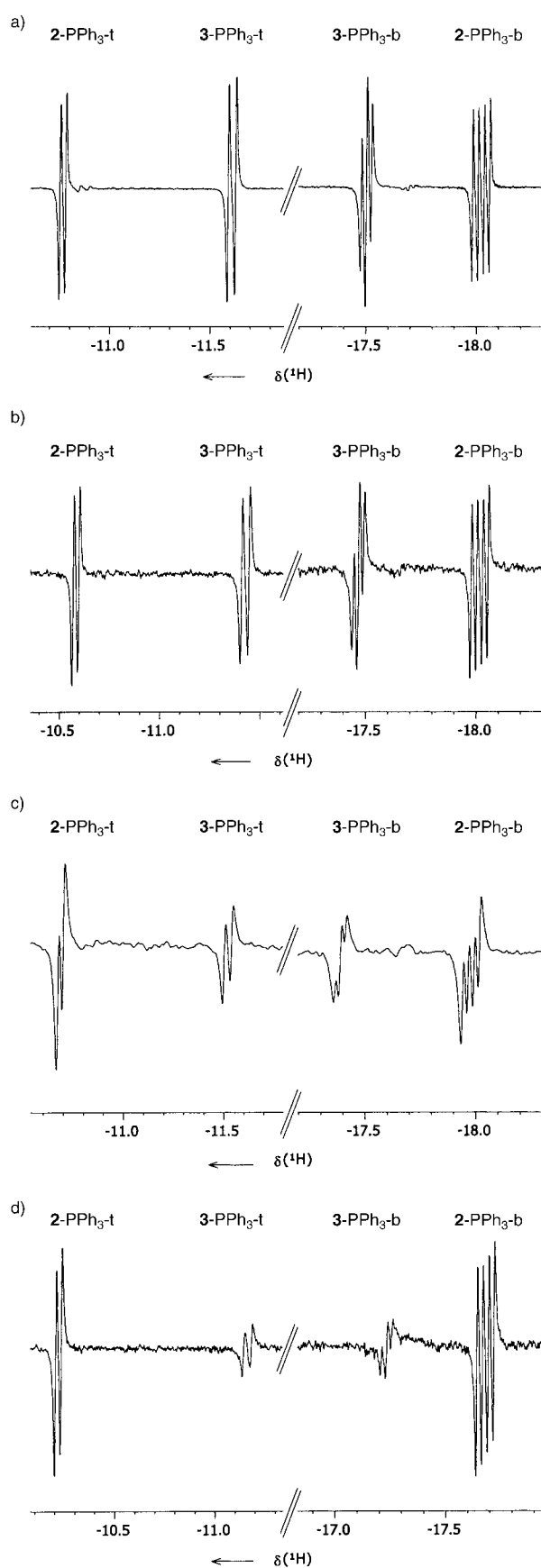

Figure 4. ¹H NMR spectra (256 scans) at constant vertical expansion showing p-H₂ enhanced peaks for 2-PPh₃ and 3-PPh₃ at 301 K in the presence of a 100-fold excess of diphenylacetylene: a) in CDCl₃, b) in [D₈]THF, c) in CD₃NO₂ (64 scans only) and d) in [D₈]toluene.
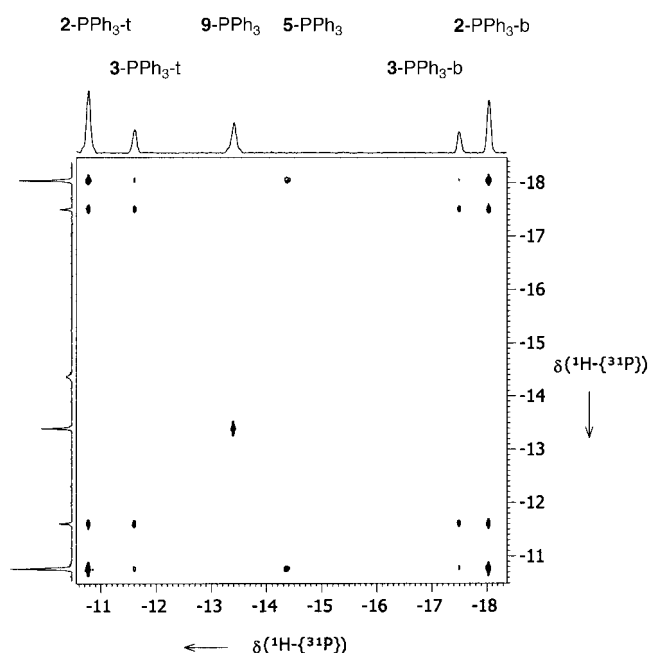
Figure 5. 2D ^{1}H-{^{31}P} EXSY spectrum (positive contour display) of a sample of **1**-PPh$_3$ in CDCl$_3$ in the presence of a 100-fold excess of diphenylacetylene at 301 K with a mixing time of 400 ms. Off-diagonal peaks arise due to chemical exchange.

[H$_2$] remains essentially constant during the run. A typical kinetic trace is shown in Figure 7b, with the associated observed rate constants at 301 K listed in Table 4. In highly polar CD$_3$NO$_2$, hydrogenation by **3**-PPh$_3$ was too fast to be followed on the NMR timescale and in contrast, in [D$_8$]toluene the low signal strengths for **3**-PPh$_3$ and **9**-PPh$_3$ precluded the observation of magnetisation transfer into the alkene.

Effect of concentration of CO, PPh$_3$ and alkyne on the hydrogenation rate: Experiments in which the concentrations of CO, PPh$_3$ and alkyne are varied at constant [H$_2$] revealed that: 1) the rate of interconversion of **2**-PPh$_3$ and **3**-PPh$_3$ into **5**-PPh$_3$ and **9**-PPh$_3$ is reduced as the concentration of free PPh$_3$ increases, 2) the interconversion between **2**-PPh$_3$ and **3**-PPh$_3$ as well as the rate of hydrogenation decreases with increase in free CO concentration and 3) halving the alkyne concentration or increasing it further has no effect on the hydrogenation rate. We note that since **2**-PPh$_3$ and **3**-PPh$_3$ correspond to minor reaction products or reaction intermediates, the excess of alkyne relative to them is always substantial.[49]

Variation of hydrogenation efficiency with [H$_2$]: When the pressure of hydrogen was decreased from 3 to 2 atm, thus reducing the [H$_2$] in solution by 33%, examination of **2**-PPh$_3$-t with a mixing time of 700 ms revealed that the ratio of the hydride peak/*cis*-stilbene product peak in the 1D EXSY spectrum decreased from 6.0:1 to 3.7:1, while on moving to 1 atm it dropped further to 1.9:1. This change in intensity corresponds to a linear decrease in reaction rate and indicates that there is a first-order dependence of the rate of product formation on the concentration of hydrogen in solution. This observation suggests that the binding of a new molecule of H$_2$ occurs before the rate-determining step in the mechanistic cycle. In order to compare the
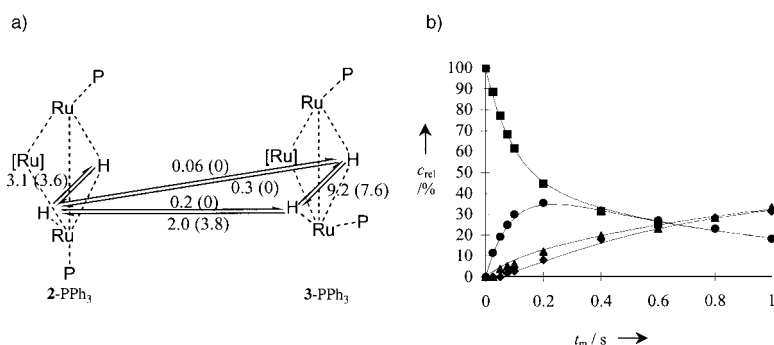

Figure 6. a) Schematic diagram showing the exchange rates in the absence (and presence) of direct hydrogenation as determined by simulation; b) Simulation (solid line) and experimental (points) trace showing exchange processes starting from site **3**-PPh$_3$-b in CDCl$_3$ at 301 K in the presence of a 100-fold excess of diphenylacetylene under conditions in which no direct hydrogenation is evident; c_{rel} indicates relative concentration and t_m represents the mixing time in the EXSY experiment. **3**-PPh$_3$-t: ●; **3**-PPh$_3$-b: ■; **2**-PPh$_3$-t: ▲; **2**-PPh$_3$-b: ◆.

Table 2. Rate constants [s^{-1}] obtained for hydride interchange in **2**-PPh$_3$ and **3**-PPh$_3$, determined under conditions where the [H$_2$] is too low for direct hydrogenation to be observed on the NMR timescale.

		284 K	289 K	296 K	301 K	307 K	312 K	317 K
2-PPh$_3$-t → **2**-PPh$_3$-b	CDCl$_3$	0.5	0.8	1.7	3.1	4.7	8.1	11.5
	[D$_8$]THF		1.2	1.9	3.7	5.8	9.0	12.6
	[D$_8$]toluene		1.6	2.6	4.2	6.9	11.0	
2-PPh$_3$-t → **3**-PPh$_3$-t	CDCl$_3$	0.003	0.01	0.05	0.2	0.3	0.6	1.1
2-PPh$_3$-t → **3**-PPh$_3$-b	CDCl$_3$	0.004	0.009		0.06	0.3		
3-PPh$_3$-t → **2**-PPh$_3$-t	CDCl$_3$	0.3	0.6	1.2	2.0	4.1	5.1	6.4
	[D$_8$]THF	0.7	0.8	1.5	2.6	4.0	6.7	
	[D$_8$]toluene		0.7	1.5	3.3	3.6		
3-PPh$_3$-b → **2**-PPh$_3$-t	CDCl$_3$		0.03	0.1	0.3	0.9	2.6	4.0
	[D$_8$]THF		0.1	0.2		1.8	4.6	9.3
	[D$_8$]toluene		0.3	0.7	0.9	4.3	8.4	
3-PPh$_3$-t → **3**-PPh$_3$-b	CDCl$_3$	1.7	3.1	5.5	9.2	14.2	22.9	
	[D$_8$]THF	4.1	6.8	10.9	17.2	24.3	30.0	

Table 3. Activation parameters for hydride interchange in **2**-PPh$_3$ and **3**-PPh$_3$ when the [H$_2$] is too low for direct hydrogenation to be observed on the NMR timescale.

Process	CDCl$_3$	[D$_8$]THF	[D$_8$]Toluene
2-PPh$_3$-t → **2**-PPh$_3$-b			
$\Delta H^{\ddagger}$ [kJ mol^{-1}]	72 ± 4	67 ± 5	60 ± 9
$\Delta S^{\ddagger}$ [J K^{-1} mol^{-1}]	1 ± 14	-12 ± 16	-33 ± 29
2-PPh$_3$-t → **3**-PPh$_3$-t			
$\Delta H^{\ddagger}$ [kJ mol^{-1}]	132 ± 19		
$\Delta S^{\ddagger}$ [J K^{-1} mol^{-1}]	175 ± 62		
2-PPh$_3$-t → **3**-PPh$_3$-b			
$\Delta H^{\ddagger}$ [kJ mol^{-1}]	136 ± 29		
$\Delta S^{\ddagger}$ [J K^{-1} mol^{-1}]	188 ± 98		
3-PPh$_3$-t → **2**-PPh$_3$-t			
$\Delta H^{\ddagger}$ [kJ mol^{-1}]	77 ± 9	54 ± 6	68 ± 1
$\Delta S^{\ddagger}$ [J K^{-1} mol^{-1}]	16 ± 30	-57 ± 19	
3-PPh$_3$-b → **2**-PPh$_3$-t			
$\Delta H^{\ddagger}$ [kJ mol^{-1}]	139 ± 16	114 ± 12	114 ± 42
$\Delta S^{\ddagger}$ [J K^{-1} mol^{-1}]	206 ± 52	133 ± 39	
3-PPh$_3$-t → **3**-PPh$_3$-b			
$\Delta H^{\ddagger}$ [kJ mol^{-1}]	65 ± 5	53 ± 3	
$\Delta S^{\ddagger}$ [J K^{-1} mol^{-1}]	-11 ± 15	-45 ± 10	

rate data for this process, the initial [H$_2$] was determined in each solvent system[50] and the true rate constants k ($k = k_{obs}/$[H$_2$]) were calculated (see Table 4).

Evidence for the pairwise nature of hydride transfer: The observation of the PHIP effect allows the examination of pairwise hydrogen exchange processes at high sensitivity. However, since this need not be the only exchange pathway,[51] a mixture of H$_2$ and D$_2$ was employed to test the mechanistic route. Since no HD containing ruthenium or organic products were observed, fully pairwise mechanisms can be deduced.

Discussion of kinetic data for hydride exchange pathways within 2-PPh$_3$ and 3-PPh$_3$: From Table 2 it can be seen that intra-isomer hydride exchange in **3**-PPh$_3$ proved to be the fastest dynamic process, with the terminal hydride moving into the bridging position at a rate of 9.2 s^{-1} in CDCl$_3$ at 301 K. The corresponding process in **2**-PPh$_3$ is slower, with a rate of 3.1 s^{-1}; on an even slower timescale inter-isomer exchange occurs, with **3**-PPh$_3$-t moving into the terminal position **2**-PPh$_3$-t at a rate of 2.0 s^{-1} and **3**-PPh$_3$-b moving into position **2**-PPh$_3$-t at a rate of 0.3 s^{-1}.

Interestingly, the rates of hydride exchange within **2**-PPh$_3$ and **3**-PPh$_3$ were unaffected (within experimental error) when the experiments were repeated with an additional atmosphere of CO. However, the rate of inter-isomer interchange from **3**-PPh$_3$ to **2**-PPh$_3$ with the hydride ligands maintaining their relative positions was reduced by approximately 25%, while the rate constants for inter-isomer exchange with hydride position interchange and interchange from **2**-PPh$_3$ to **3**-PPh$_3$ with hydride position retention were dramatically reduced. All six of these processes were unaffected by the addition of PPh$_3$.

From Table 3 it can be seen that the bridge ↔ terminal hydride exchanges in **2**-PPh$_3$ and **3**-PPh$_3$ are characterised by relatively small enthalpies of activation (72 ± 4 kJ mol^{-1} in CDCl$_3$ for **2**-PPh$_3$) and entropies of activation, which are close to zero or slightly negative. The activation parameters are
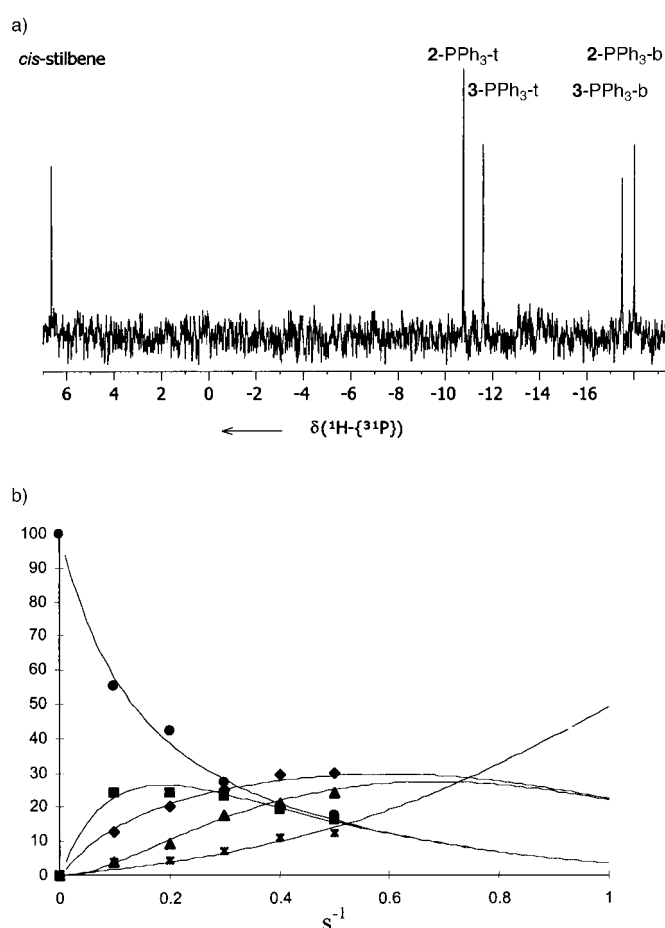

Figure 7. a) 1D p-H$_2$-enhanced ^{1}H-{^{31}P} EXSY spectrum recorded in CDCl$_3$ at 301 K on a sample containing a 100-fold excess of diphenylacetylene. The resonance for **3**-PPh$_3$-t was excited and the results obtained with a mixing time of 700 ms are displayed. b) Simulated (solid line) and experimental (points) data for the corresponding composition versus time profile. **3**-PPh$_3$-t: ●; **3**-PPh$_3$-b: ■; **2**-PPh$_3$-t: ▲; **2**-PPh$_3$-b: ◆; *cis*-stilbene: *.

clearly too small to indicate ligand loss in the rate-determining step. A concerted motion of hydride and carbonyl ligands has been proposed to account for hydride interchange in

Table 4. Rate constants (k_{obs} [s^{-1}] and k [dm^3 mol^{-1} s^{-1}]) for the hydride transfer from **2**-PPh$_3$, **3**-PPh$_3$, **9**-PPh$_3$, **2**-PMe$_2$Ph, **4**-PMe$_2$Ph and **9**-PMe$_2$Ph into *cis*-stilbene at 301 K, in which $k_{obs} = k$ [H$_2$].

	CDCl$_3$	CDCl$_3$/CD$_3$NO$_2$ 1:1	CD$_3$NO$_2$	[D$_8$]Toluene	[D$_8$]THF
2-PPh$_3$					
k_{obs}	0.05	0.08	0.13	0.02	0.08
k	1.4	1.5	1.9	1.1	1.3
3-PPh$_3$					
k_{obs}	0.31	0.46	fast	slow	0.58
k	9.4	8.9	fast	slow	9.5
9-PPh$_3$					
k_{obs}	0.07	0.09	0.10	slow	0.10
k	2.2	1.8	1.5	slow	1.6
2-PMe$_2$Ph					
k_{obs}	0.25				
k	7.6				
4-PMe$_2$Ph					
k_{obs}	0.05				
k	1.5				
9-PMe$_2$Ph					
k_{obs}	0.18				
k	5.4				

[Os₃(μ-H)(H)(CO)₁₁] and its derivatives,[52] while a concerted merry-go-round mechanism has been suggested for [Fe₃-(CO)₁₂₋ₓ(L)ₓ] (x = 1–3).[53] Mechanisms involving Ru–Ru bond cleavage, in either homolytic[54] or heterolytic[55] fashion, are also possible. However, since the homolytic mechanism would quench the observed *p*-H₂ enhancement[56] we conclude it cannot account for our observations. We believe that hydride interchange occurs through rate-determining metal–metal bond heterolysis, in an analogous manner to that previously deduced for [Ru₃(μ-H)(H)(CO)₁₀(PMe₂Ph)₂];[30] this is further supported by the similarities in the enthalpies of activation for the two systems. The lack of a substantial solvent effect has previously been explained for **1**-PPh₃ by the bulk of the PPh₃ ligand preventing the solvent from interacting,[30] and the same is suggested here. Exchange would then proceed by either a Berry psuedorotation or formation of an η^2-H₂ ligand (see Scheme 1).[56]
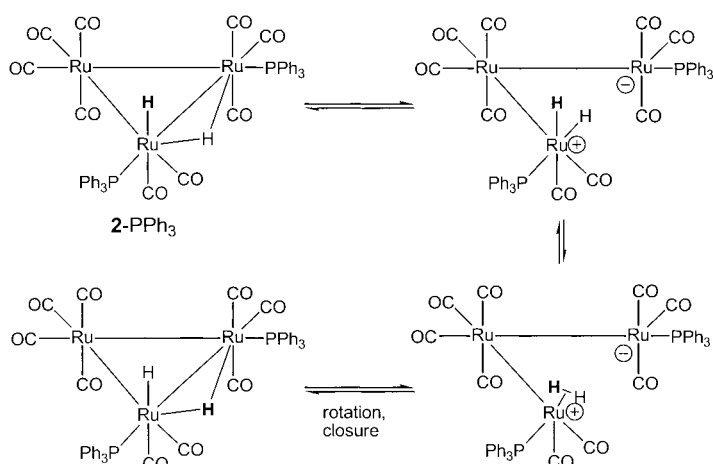
Scheme 1. Proposed intra-isomer hydride exchange pathway for **2**-PPh₃.

Inter-isomer exchange from **2**-PPh₃ to **3**-PPh₃, both maintaining and swapping hydride positions, and exchange from **3**-PPh₃ to **2**-PPh₃ with hydride position interchange, all have large positive values for both the entropy and enthalpy of activation (e.g. $\Delta H^{\pm} = 139 \pm 16$ kJ mol⁻¹ and $\Delta S^{\pm} = 206 \pm 52$ J K⁻¹ mol⁻¹ for the latter process in CDCl₃). This indicates that ligand loss occurs prior to, or in, the associated rate-determining step. Since all these processes were inhibited by CO and unaffected by phosphine, it can be concluded that CO dissociation features in these processes. Subsequent steps, including phosphine migration and re-coordination of CO, are necessary before the final product is formed.

Significantly, inter-isomer exchange from **3**-PPh₃ to **2**-PPh₃ while maintaining hydride positions exhibits a $\Delta H^{\pm}$ value of 77 ± 9 kJ mol⁻¹ and a $\Delta S^{\pm}$ of 16 ± 30 J K⁻¹ mol⁻¹ in CDCl₃ and shows a considerable solvent effect. This process was also slowed down by CO addition. Clearly, this exchange process involves a substantially different rate-determining step from the preceding processes. We therefore suggest that both CO loss and Ru–Ru bond heterolysis occur prior to the rate-determining step. This accounts for the effect of solvent and the similarity in activation parameters to those for exchange

within **2**-PPh₃ and within **3**-PPh₃.[30, 57] This picture is, however, further complicated by the need for subsequent phosphine migration and closure.

Role of 2-PPh₃ and 3-PPh₃ in the hydrogenation of diphenylacetylene: The results obtained show that **3**-PPh₃ is the most active species, with a corrected hydrogenation rate of 9.4 dm³ mol⁻¹ s⁻¹ in CDCl₃ at 301 K, followed by **2**-PPh₃ and **9**-PPh₃ which have similar activities (the rates are 1.4 dm³ mol⁻¹ s⁻¹ and 2.2 dm³ mol⁻¹ s⁻¹, respectively). In Figure 4 we demonstrated that the solvent seems to play a role in controlling the rate of hydrogenation. However, as shown in Table 4, once the k_{obs} values are corrected for the hydrogen concentration, the true hydrogenation rate constants in all solvents are very similar (for instance, the hydrogenation rates obtained for **2**-PPh₃ remain between 1.1 and 1.9 dm³ mol⁻¹ s⁻¹ in the five solvents investigated). The effect of the solvent therefore arises as a consequence of solvent polarity controlling the equilibrium between the active hydride species and the unreacted precursor. In the case of **1**-PPh₃, the active species **2**-PPh₃ and **3**-PPh₃ are formed to a greater extent in higher polarity solvents;[58] this leads to the apparently faster "visible" rate. Based on previous work, this equilibrium has been rationalised in terms of the promotion of the Ru–Ru bond heterolysis step that allows access to the active H₂ addition products.[30, 33, 57]

Collectively, these data support the suggestion that interchange between **2**-PPh₃ and **3**-PPh₃ involves CO loss and indicate that the trapping of the intermediate by alkyne leads to hydrogenation. When the reaction was carried out in the presence of acetonitrile, a coordinating solvent, the intensity of the hydride signals decreased greatly in accordance with the expected competition between the substrate and CH₃CN for the vacant site that is formed by CO loss.

Interestingly, the ratio of the rate constants $(k_{3\text{-PPh}_3 \to 2\text{-PPh}_3})/(k_{2\text{-PPh}_3 \to 3\text{-PPh}_3})$ as determined from exchange data in the presence of alkyne equates to a sixfold preponderance of **2**-PPh₃ over **3**-PPh₃ in solution. This situation closely matches the relative intensities of the hydride resonances that were observed in the absence of substrate. However, in the spectra recorded in the presence of alkyne and H₂, the hydride signal intensities of **2**-PPh₃ and **3**-PPh₃ are comparable. This effect therefore arises because **3**-PPh₃ is the most rapid hydrogenation catalyst (as shown by the kinetic data in Table 4) and the degree of enhancement of the associated resonances is larger than that for **2**-PPh₃ because the *p*-H₂ spin state is more efficiently populated. While both **2**-PPh₃ and **3**-PPh₃ interconvert directly into **5**-PPh₃, only **3**-PPh₃ has been observed to rearrange into **9**-PPh₃, with the rates for all the processes reducing with increasing [PPh₃]. It can therefore be concluded that both **5**-PPh₃ and **9**-PPh₃ are formed through PPh₃ loss. An empirical formula for **5**-PPh₃ would therefore correspond to [Ru₃(H)₂(CO)₉(PPh₃)]. Since this complex exhibits only one hydride resonance, it must possess equivalent hydride ligands, with the chemical shifts of $\delta = -14.35$ ppm indicating a bridging arrangement. The related 46 electron cluster [Ru₃(μ-H)₂(CO)₁₀] has been reported to yield a hydride resonance at $\delta = -13.6$ ppm,[59] while the corresponding resonance in [Os₃(H)₂(CO)₉(PPh₃)] appears at $\delta =$

−10 ppm;[60] these reports would support the structural assignment. However, [Ru₃(H)₂(CO)₉(PPh₃)] has been suggested by Leadbeater to yield a hydride signal at $\delta =$ −17.8 ppm.[59] Nonetheless, we still feel that complex **5**-PPh₃ most likely corresponds to the co-ordinatively unsaturated 46 electron species [Ru₃(μ-H)₂(CO)₉(PPh₃)] with equivalent hydrides.[27]

The effect of hydrogenation on the rate of exchange between the hydride sites of **2**-PPh₃ and **3**-PPh₃ is also noteworthy (Figure 6a). As mentioned above, **3**-PPh₃ undergoes the fastest transfer of magnetisation into the alkene hydrogenation product, and the interconversion of **2**-PPh₃ to **3**-PPh₃ has been shown to involve CO loss. Under conditions in which direct transfer into the alkene is visible on the NMR timescale, the intra-isomer hydride exchange rate for **3**-PPh₃ reduces from 9.2 to 7.6 s⁻¹, while the corresponding process for **2**-PPh₃ speeds up slightly from 3.1 to 3.6 s⁻¹. Inter-isomer exchange from **3**-PPh₃ to **2**-PPh₃ with retention of the same relative hydride position also speeds up from 2.0 to 3.8 s⁻¹, but the remaining three interchange pathways are totally quenched. Since these three processes involve CO loss, alkyne binding must totally block CO re-coordination under these conditions and hence prevent their completion. These data indicate that since the overall rate of exchange from **2**-PPh₃ to **3**-PPh₃ decreases from 0.26 s⁻¹ to zero during hydrogenation, alkyne trapping by **2**-PPh₃ must be essentially quantitative. In the opposite process, the overall rate of exchange from **3**-PPh₃ to **2**-PPh₃ increases from 2.3 to 3.8 s⁻¹, indicating that alkyne binding to **3**-PPh₃ is reversible and much less efficient than that to **2**-PPh₃. Isomer **3**-PPh₃ is also better able to lose CO than

2-PPh₃ and, hence, has a higher overall hydrogenation activity.

From these experiments, the mechanism of hydrogenation shown in Scheme 2 has been devised. The CO *trans* to the terminal hydride would be the most likely ligand to dissociate in this process due to the labialising effect of the terminal hydride and as the Ru−C axial bonds are longer, and hence weaker, than equatorial Ru−C bonds.[41] The bridging hydride ligand would then transfer to the organic substrate, since the terminal hydride is blocked by the *cis* phosphine and carbonyl ligands. The terminal hydride would instead move to a bridging coordination (intermediate **A** in Scheme 2). The dependence of the rate on the concentration of hydrogen indicates that prior to elimination of the alkene, another molecule of H₂ must add, but the pairwise nature of the process requires that the original terminal hydride ligand be transferred to the substrate. The reaction is then completed by the dissociation of the newly formed *cis*-stilbene, the splitting of the new H₂ molecule to give a terminal and bridging hydride and either re-coordination of a new alkyne molecule to repeat the cycle, or of CO to regenerate **2**-PPh₃ or **3**-PPh₃. Related H₂ addition to Ru and Os dihydride-containing clusters prior to H₂ exchange has been suggested previously.[61] Only *cis*-stilbene, the kinetic product, is observed in this reaction, with no isomerisation[62] evident after 48 hours. Given the steric bulk of diphenylacetylene and of triphenylphosphine, which are both located on the same Ru atom, this is consistent with essentially irreversible hydrogen transfer and the failure to bind *cis*-stilbene in a subsequent cycle. In addition to the main pathway, a minor process involving loss of PPh₃ from **2**-PPh₃ and **3**-PPh₃ competes with CO loss and
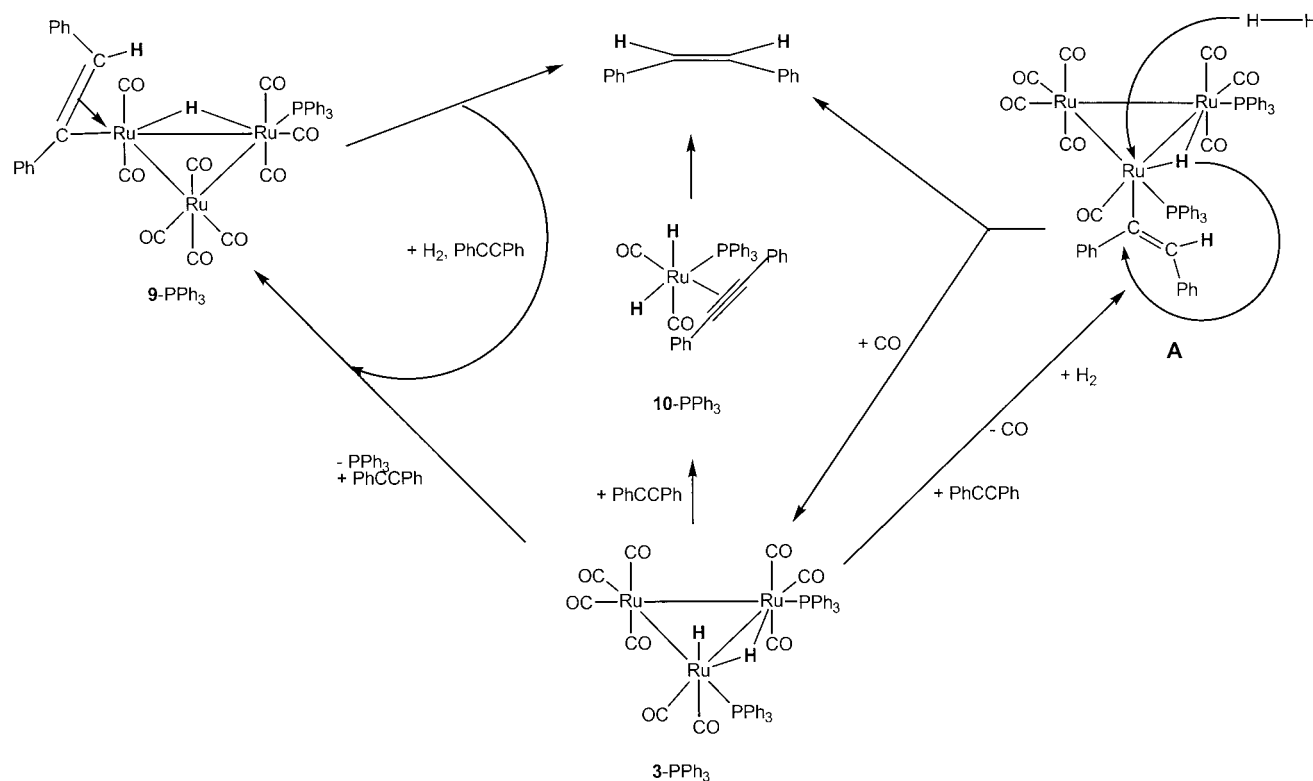
Scheme 2. Proposed hydrogenation pathway for **3**-PPh₃.

leads to the formation of inactive **5**-PPh₃ and slower hydrogenation via **9**-PPh₃, a μ_1-η^2-PhC≡CHPh resting state with a relatively long lifetime.

Effect of substrate identity: The hydrogenation of the substrates listed in Table 5 by **1**-PPh₃ was studied in CDCl₃ at 296 K. The same basic reactivity pattern as with diphenylacetylene was observed, but the relative size of the

Table 5. Effect of substrates and detection of fragmentation products during catalytic hydrogenation by **1**-PPh₃.

Substrate	Solvent	Relative enhancement		Species **9** observed	δ ¹H for **10**
		2-PPh₃	**3**-PPh₃		
PhC≡CPh	CDCl₃	5	32	Yes	
PhC≡CMe	CDCl₃	2.5	4	Yes	
trans-stilbene	CDCl₃	2.5	4	No	
styrene	C₆D₆	1	1	No	− 6.54, − 7.22
3-nitro-styrene	C₆D₆	1	1	No	− 6.65, − 7.35
PhC≡CH	C₆D₆	1.5	1	No	− 8.57, − 9.46
Me₂C≡CH	CDCl₃	2.5	2	No	− 7.34, − 8.21

hydride resonance enhancements for **2**-PPh₃ and **3**-PPh₃ varied with substrate as indicated. The data show that diphenylacetylene corresponds to the most active substrate. In the case of 1-phenyl-1-propyne, additional resonances were observed for a product containing a μ_1-η^2-MeC≡CHPh unit at $\delta = - 13.46$ and 7.34 ppm. This species is directly analogous to **9**-PPh₃.

Evidence for fragmentation during catalysis: When styrene was employed as the substrate in C₆D₆ at 296 K, signals for **2**-PPh₃ and **3**-PPh₃ were visible. In addition, two new signals were detected in the *p*-H₂ ¹H NMR spectrum at $\delta = - 6.54$ and − 7.22 ppm (see Figure 8), both appearing as doublets of antiphase doublets and assigned to species **10**-PPh₃ (see Figure 1). The resonance of **10**-PPh₃ at $\delta = - 6.54$ ppm showed
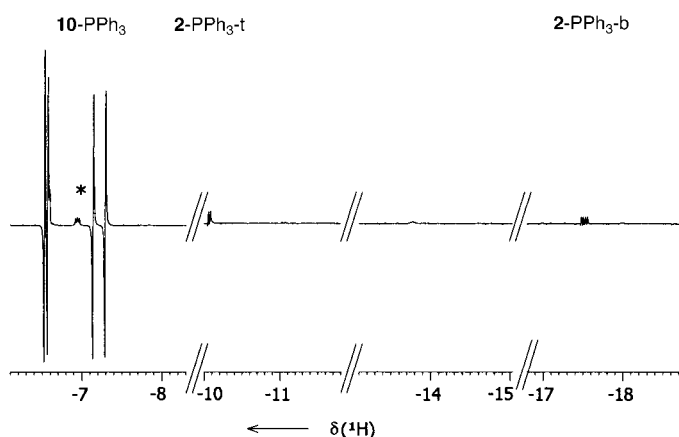
a $^2J_{HP}$ of 15 Hz (to a ³¹P resonating at $\delta = 44.91$ ppm) that is indicative of a *cis* hydride-phosphine orientation, while the resonance at $\delta = - 7.22$ ppm contained a 62 Hz splitting due to coupling to the same ³¹P nucleus; this requires a *trans* hydride-phosphine orientation. The characteristics of **10**-PPh₃ are similar to those reported for [Ru(H)₂(CO)₃(PPh₃)],[36] a known fragmentation product from this cluster family,[62] but differ slightly in terms of their absolute chemical shift. To fully characterise **10**-PPh₃, a sample of **1**-PPh₃-¹³C was employed as the precursor. The resonances for **10**-PPh₃-¹³C now showed additional couplings to ¹³C and, using ¹H-¹³C-{³¹P} HMQC, two carbonyl ¹³C resonances were located for this species at $\delta = 197.1$ and 199.0 ppm in C₆D₆ at 296 K. When the associated spectral parameters were optimised for each resonance, a high-resolution experiment revealed that both of them were doublets in the ¹³C dimension with a ¹³C – ¹³C coupling of 7 Hz indicative of the presence of only two carbonyl ligands in a *cis*-arrangement (see Supporting Information).[41] This supports the structure for **10**-PPh₃ shown in Figure 1. Interestingly, no evidence for direct hydrogenation via **10**-PPh₃ was observed on the NMR timescale, which suggests that hydride transfer to the alkene in [Ru(H)₂-(CO)₂(styrene)(PPh₃)] is relatively slow.

Surprisingly, when **1**-PPh₃ was treated with *p*-H₂ and styrene in CDCl₃, the resonances for **10**-PPh₃ were five times less intense than those observed in C₆D₆, while the resonances for **2**-PPh₃ were 25 % larger and those for **3**-PPh₃ remained unchanged. This indicates that the formation of cluster-based dihydride intermediates is facilitated by polar solvents, whilst fragmentation is facilitated by nonpolar solvents. The kinetic studies reveal, however, that cluster-based hydrogenation dominates over fragment-based routes. Thus, polar solvents should be utilised to increase the rate of catalytic hydrogenation.

Further support for the identity of **10**-PPh₃ was obtained when the same experiments were repeated with 3-nitrostyrene as the substrate. Signals for the corresponding species [Ru(H)₂(CO)₂(3-nitrostyrene)(PPh₃)] were now visible at $\delta = - 6.65$ and − 7.35 ppm. On using phenylacetylene, the corresponding product's hydride resonances appeared at $\delta = - 8.57$ and − 9.46 ppm, while with 3,3-dimethyl-1-butyne they shifted to $\delta = - 7.34$ and − 8.21 ppm. This species has therefore been unambiguously shown to contain the substrate (see Figure 1) and clearly corresponds to [Ru(H)₂(CO)₂(L)(PPh₃)], in which L = styrene, 3-nitrostyrene, phenylacetylene and 3,3-dimethyl-1-butyne (see Table 5).

Effect of the degree of substitution in the precursor [Ru₃-(CO)₁₂₋ₓ(PPh₃)ₓ] ($x = 1 – 3$) on hydrogenation activity: When the mono-substituted cluster **6**-PPh₃ is used as the catalytic precursor, hydrogenation of diphenylacetylene proceeds exclusively via **9**-PPh₃. On a per mole basis, the tris-substituted cluster **8**-PPh₃ showed lower overall activity than **1**-PPh₃, since phosphine loss is less efficient and hence less of the key dihydride species are produced.[7] Under the same conditions, [Ru₃(CO)₁₂] proved inactive, an effect that has been observed previously.[64] Even when [Ru₃(CO)₁₂] and two equivalents of phosphine were combined in situ, only a very slow reaction results at 301 K, due to the slow initial substitution of CO by PPh₃. When **6**-PPh₃ and **8**-PPh₃ were used as the precursors in

Figure 8. *p*-H₂-enhanced ¹H NMR spectrum (256 scans) of **1**-PPh₃ obtained in C₆D₆ at 296 K in the presence of a 100-fold excess of styrene. Enhanced resonances due to the *cis*, *trans* isomer of **10**-PPh₃ are clearly visible. The peak marked with a * is due to the corresponding *cis*, *cis* isomer.[40]

C_6D_6 with styrene as the substrate, both cluster- and fragment-based dihydride products were detected, but at ten times lower hydride signal intensities than when **1**-PPh$_3$ was employed.

It can therefore be concluded that the activity of the bis-substituted cluster towards hydrogenation is much greater than that of the mono- and tris- substituted analogues. This situation arises due to the higher resulting concentrations of the dihydride-substituted cluster products and to the availability of two different hydrogenation routes involving CO and phosphine loss that subsequently enable hydrogenation to take place.

Effect of phosphine on the rate of hydrogenation of diphenylacetylene: When **1**-PMe$_2$Ph was used as the catalytic precursor in the presence of a 100-fold excess of diphenylacetylene at 296 K, the additional enhancement of the hydride resonances of **2**-PMe$_2$Ph and **4**-PMe$_2$Ph over that seen in the absence of substrate was only a factor of 2 for the former and 2.5 for the latter. In this experiment, enhanced signals due to the hydrogenation product *cis*-stilbene were observed, but no vinyl hydride species was detected. The hydrogenation activity of **2**-PMe$_2$Ph and **4**-PMe$_2$Ph was monitored in a quantitative fashion by the EXSY method and rate constants were determined (see Table 4). Each isomer of the PMe$_2$Ph-substituted cluster is more active than its PPh$_3$ counterpart, but since no **3**-PMe$_2$Ph is formed, the overall activity of **1**-PPh$_3$ is greater than that of **1**-PMe$_2$Ph.

Slower catalysis was again evident when the tris-substituted cluster was employed. However, when the mono-substituted cluster **6**-PMe$_2$Ph was utilised, a vinyl species **9**-PMe$_2$Ph was formed, which proved to be more active than **9**-PPh$_3$. On moving to conditions that favoured catalysis by fragmentation, all three PMe$_2$Ph clusters behaved in the same manner as their PPh$_3$ analogues, but the relative sizes of the corresponding hydride signals were at least 20 times smaller. Fragmentation reactions of the products of H$_2$ addition to **1**-PMe$_2$Ph are therefore less efficient than their PPh$_3$ analogues. The NMR data for these products are listed in Table 1.

When **1**-PMe$_3$ was examined with diphenylacetylene in CDCl$_3$ at 301 K, the signals observed for the hydride ligands in **2**-PMe$_3$ and **4**-PMe$_3$ were both considerably enhanced over the situation without substrate. However, their actual size was still very small, indicating that the extent of hydrogen uptake by **1**-PMe$_3$ is very low. However, the *cis*-stilbene to hydride signal intensity ratio exceeded 10:1, while that seen for **1**-PMe$_2$Ph was approximately 1:1. This indicates that **2**-PMe$_3$ and **4**-PMe$_3$ hydrogenate diphenylacetylene very rapidly. However, the small size of the associated hydride resonances precluded quantification of the rate.

On moving to **1**-PCy$_3$, the signals observed for **2**-PCy$_3$ proved to be substantially larger than those observed with any other phosphine, and a new vinyl species corresponding to **9**-PCy$_3$ was observed with similar spectral characteristics to those seen for **9**-PPh$_3$. In addition, significant fragmentation was evident. The first fragmentation product yielded enhanced hydride resonances at $\delta = -7.03$ and -8.12 ppm, which suggested that **10**-PCy$_3$ with a bound diphenylacetylene ligand was formed. A second hydride resonance was also observed at $\delta = -7.99$ ppm, which was substantially increased

in size when **1**-PCy$_3$-^{13}C was used as the precursor. The two hydride ligands in this species can therefore be deduced to be chemically equivalent, with the ^{13}C label breaking the symmetry and allowing the detection of the *cis–cis* isomer of [Ru(H)$_2$(CO)$_2$(PCy$_3$)(substrate)] (**11**-PCy$_3$).[65] Although the formation of relatively large amounts of these active species was indicated, no evidence for direct magnetisation transfer into *cis*-stilbene could be obtained. This suggests that hydrogen uptake by **1**-PCy$_3$ is very effective, but hydrogenation by the resulting species is slow at 301 K. This is consistent with the fact that the ratio of the alkene proton resonance to the cluster hydride signal is 50% lower than when **1**-PMe$_2$Ph is used as the precursor. On using the mono-substituted analogue **6**-PCy$_3$, the formation of the corresponding vinyl species **9**-PCy$_3$ was observed, but the rate of hydrogenation from this species proved to be too slow for determination. This indicates that **9**-PCy$_3$ is less prone to alkene loss than **9**-PPh$_3$ and **9**-PMe$_2$Ph.

These data show that the steric and electronic properties of the phosphine influence the hydrogenation mechanism. Increasing the steric bulk of the phosphine ligand initially results in a greater abundance of the active dihydride species and the possibility of hydrogenation both via the formation of **9** (phosphine loss) and directly (CO loss). However, if the steric bulk is too large, as can be seen when PCy$_3$ is used, fragmentation is encouraged and this reduces the overall catalytic activity. Furthermore, when the activities of **2** are compared, it can be seen that the smaller phosphines yield fastest direct hydrogen transfer into the alkyne, but the most active of the dihydride isomers, **3**, is only observed with less basic phosphines. It is therefore clearly difficult to identify the "ideal phosphine ligand" for use in these reactions. What is required is a phosphine of intermediate steric bulk, to optimise the trade-off between the amount of active species formed and the rate of elimination, and one that is not a strong donor to enable the formation of **3**, the most active species for hydrogenation.

Conclusion

The addition of hydrogen to phosphine (L) substituted clusters [Ru$_3$(CO)$_{12-x}$(L)$_x$], where $x = 1-3$, and their subsequent reactivity towards hydrogenation reactions have been investigated. It has been shown that the bis-substituted clusters are the most active, with CO loss leading to hydrogen addition and the formation of up to three different isomers in solution, which exhibit complex dynamic behaviour. The activation parameters determined for [Ru$_3$(H)(μ-H)-(CO)$_9$(PPh$_3$)$_2$] indicate that intra-isomer hydride exchange occurs through Ru–Ru bond heterolysis in the rate-determining step, followed by dihydrogen formation, rotation about the associated H–H bond and closure (see Scheme 1). Three of the intra-isomer exchange pathways were shown to involve CO loss prior to the rate-determining step, with the trapping of the associated vacant site by alkyne being crucial for catalysis. The corresponding mono-substituted clusters were less active towards the initial addition of hydrogen, and formed only one dihydride product, while the tris-substituted

clusters added hydrogen through loss of phosphine to form the same species seen with [Ru$_3$(CO)$_{10}$(L)$_2$], but to a lesser extent.

All observed clusters were shown to be active catalysts for hydrogenation, which was directly monitored and the reaction mechanism elucidated (see Scheme 2). After initial hydrogen addition, either fragmentation catalysis or catalysis by intact clusters follows. The choice of route depends on the substrate and the solvent, with intact cluster catalysis preferred in polar solvents and fragmentation to [Ru(H)$_2$(CO)$_2$(PPh$_3$)(substrate)] being facilitated by nonpolar solvents. If the cluster stays intact, CO loss or slower phosphine loss lead to hydrogenation, with the substrate binding to the vacant site. This process shows a first-order dependence on the [H$_2$], which requires H$_2$ to coordinate before the product is eliminated. In all cases, catalysis by a route involving an intact cluster showed much greater activity than that involving a mononuclear counterpart.

Within each phosphine family, the bis-substituted cluster was found to be the most active hydrogenation catalyst. This is attributed to such species having access to more active dihydride forms, and hence greater reaction flexibility. In the case of the mono-substituted precursor [Ru$_3$(CO)$_{11}$(L)], only one isomer of [Ru$_3$(H)(μ-H)(CO)$_{10}$(L)] is formed, which loses CO to form the relatively stable species [Ru$_3$(μ,η^2-vinyl)(μ-H)(CO)$_{10}$(L)]. When the tris-substituted clusters act as catalytic precursors, phosphine loss yields the hydrogen addition products by a substantially less favourable reaction pathway.

The three isomers of the hydrogen addition products formed by the bis-substituted precursor were observed to have significantly different activities towards hydrogenation, with the same trend observed within each phosphine family. Interestingly, the minor isomer **3** is the most active, with a hydrogenation rate for **3**-PPh$_3$ of 9.4 dm^3 mol^{-1} s^{-1} in CDCl$_3$ at 301 K. The major isomer **2** is less active, with a similar hydrogenation rate to that of the vinyl species **9** for PPh$_3$ (the rates for **2**-PPh$_3$ and **9**-PPh$_3$ are 1.4 and 2.2 dm^3 mol^{-1} s^{-1} in CDCl$_3$ at 301 K, respectively). The least abundant isomer, **4**, proved to be the slowest catalyst. Structures for these species are listed in Figure 1.

The steric and electronic properties of the phosphine contained in [Ru$_3$(H)(μ-H)(CO)$_9$(L)$_2$] have also been shown to play an important role. Smaller phosphines do not allow access to the catalytic pathway that involves phosphine loss and the formation of the associated vinyl-based intermediate **9**, while very large phosphines lead to fragmentation, which decreases the overall rate of catalysis. In turn, electron-donating phosphines do not form the most active isomer of the initial hydrogen addition products and hence have lower catalytic activity. Therefore, clusters containing phosphines of intermediate steric properties and that are not strongly basic, such as PPh$_3$, are optimum for hydrogenation.

Experimental Section

General methods and chemicals: All reactions were carried out under nitrogen using glove box, high-vacuum or Schlenk line techniques.

Subsequent purifications were carried out without precautions to exclude air. Triphenylphosphine, dimethylphenylphosphine, trimethylphosphine, diphenylacetylene, 1-phenyl-1-propyne, 3,3-dimethyl-1-butyne, phenylacetylene, *trans*-stilbene, *cis*-stilbene, styrene, 3-nitrostyrene (Aldrich), tricyclohexylphosphine (Fluka), [Ru$_3$(CO)$_{12}$] (Strem Chemicals), hydrogen (99.99%, BOC) and ^{13}CO (99.9%) were used as received. Tetrahydrofuran (THF) was dried over sodium and distilled under nitrogen prior to use, while hexane and dichloromethane were used as received. The clusters [Ru$_3$(CO)$_{12-x}$(L)$_x$], L = PPh$_3$ and PMe$_2$Ph, x = 1–3, PMe$_3$, x = 2 and PCy$_3$, x = 1 and 2 were prepared according to a literature radical-ion-initiated method[66] and purified on a silica column with hexane:dichloromethane (80:20) as the eluent. Labelling of [Ru$_3$(CO)$_{12}$] with ^{13}CO was achieved by stirring a solution of the cluster (100 mg) in dry THF for 72 hours under an atmosphere of ^{13}CO, as reported previously.[67] This procedure was repeated three times, after which mass spectrometry investigations revealed that the extent of ^{13}CO labelling was essentially 100%.

All NMR solvents (Apollo Scientific) were dried using appropriate methods and degassed prior to use. The NMR measurements were made by using NMR tubes fitted with Young Teflon valves and solvents were added by vacuum transfer on a high-vacuum line. For the parahydrogen-induced polarisation (PHIP) experiments, hydrogen enriched in the *para* spin state was prepared by cooling H$_2$ to 77 K over a paramagnetic catalyst (Fe$_2$O$_3$ or activated charcoal) by using the two systems described previously.[68] All NMR studies were carried out with sample concentrations of approximately 1 mM and spectra were recorded on a Bruker DRX-400 spectrometer with ^{1}H at 400.1, ^{31}P at 161.9 and ^{13}C at 100.0 MHz. ^{1}H NMR chemical shifts are reported in ppm relative to residual ^{1}H signals in the deuterated solvents ([D$_5$]benzene δ = 7.13 ppm, [D$_7$]toluene δ = 2.13 ppm, CHCl$_3$ δ = 7.27 ppm, [D$_7$]THF δ = 1.73 ppm and [D$_2$]nitromethane δ = 4.33 ppm), ^{31}P NMR in ppm downfield of an external 85% solution of phosphoric acid and ^{13}C NMR relative to [D$_6$]benzene (δ = 128.0 ppm), [D$_8$]toluene (δ = 21.3 ppm) and CDCl$_3$ (δ = 77.05 ppm). Modified COSY, HMQC and EXSY pulse sequences were used as previously described.[22]

Dynamic methods used to study hydride exchange in [Ru$_3$(H)(μ-H)-(CO)$_9$(PPh$_3$)$_2$] (2-PPh$_3$ and 3-PPh$_3$): In order to monitor hydride ligand exchange in **2**-PPh$_3$ and **3**-PPh$_3$, a series of 2D gradient assisted EXSY spectra were recorded.[22] Runs were carried out in the presence of a 100-fold excess of diphenylacetylene, which enabled sufficient signal intensity for **3**-PPh$_3$ to be observed. The sample was shaken immediately prior to each run to re-establish the parahydrogen equilibrium in solution and data acquisition did not begin until 3 minutes after sample insertion. In a typical run, data were collected at selected temperatures for a series of mixing times τ (usually 25, 50, 75, 100, 200, 400 and 600 ms). The sum of the integrals of the diagonal peak areas for a given hydride location and the cross-peak areas arising from exchange were normalised to 100%. The rate of site exchange was then determined by simulation; the change in intensity of the signal at a given hydride position (100 when τ = 0) was modelled as a function of τ.[69] The peak intensities were calculated for 0.01 s intervals from 0.01 s to τ_{max} and those for each experimentally observed time were then compared with the experimental values by means of a minimised linear-least-squares difference analysis. The associated rate constants were varied until the sum of the squares of the difference between measured and simulated points was minimised. Rate constants obtained in this way were multiplied by a factor of two to take into account the analysis method.[70] The kinetic model utilised in these simulations is presented in the Supporting Information.

Hydrogenation studies: Spectra were acquired immediately after exposing the sample to hydrogen and introducing it into the probe in order to monitor only the initial hydrogenation reaction. The results were modelled allowing for hydride exchange and hydride transfer into the corresponding hydrogenation product.

To determine hydrogen concentrations in solution, an exact pressure of 3.0 atmospheres of H$_2$ was introduced into an NMR tube containing the appropriate deuterated solvent (1 cm^3) and a marker solvent (1 mm^3) with ^{1}H NMR resonances clearly distinct from that of the deuterated solvent and of the H$_2$ peak. For the NMR solvents CDCl$_3$, CD$_3$NO$_2$, [D$_8$]toluene and [D$_8$]THF, the marker solvents were toluene, benzene, ethanol and chloroform, respectively. Since the amount of the marker was known, integration of the H$_2$ peak and that due to the marker enabled the concentration of dissolved H$_2$ to be determined.

[1] For example, see: a) *Transition Metal Clusters* (Ed.: B. F. G. Johnson), Wiley, Chichester (UK), **1980**; b) *Metal Clusters in Chemistry* (Eds.: P. Braunstein, L. A. Oro, P. R. Raithby), Wiley-VCH, New York, **1999**; c) P. J. Dyson, J. S. McIndoe, *Transition Metal Carbonyl Cluster Chemistry*, Gordon and Breach, Amsterdam, **2000**.

[2] For example see, *Catalysis by Di- and Polynuclear Metal Cluster Complexes* (Eds.: R. D. Adams, F. A. Cotton), Wiley-VCH, New York, **1998**.

[3] B. F. G. Johnson, J. Lewis, M. Gallup, M. Martinelli, *Faraday Discuss.* **1991**, *92*, 241.

[4] a) R. D. Adams, in *The Chemistry of Metal Cluster Complexes* (Eds.: D. F. Shriver, H. D. Kaesz, R. D. Adams), Wiley-VCH, New York, **1990**; b) M. Castiglioni, R. Giordano, E. Sappa, *J. Organomet. Chem.* **1987**, *319*, 167.

[5] For example, see: a) T. Kondo, M. Akazome, Y. Tsuji, Y. Watanabe, *J. Org. Chem.* **1990**, *55*, 1286; b) N. Chatani, Y. Ie, F. Kakiuchi, S. Murai, *J. Org. Chem.* **1997**, *62*, 2604; c) Y. Ishii, N. Chatani, F. Kakiuchi, S. Murai, *Organometallics* **1997**, *16*, 3615; d) N. Chatani, Y. Ishii, Y. Ie, F. Kakiuchi, S. Murai, *J. Org. Chem.* **1998**, *63*, 5129.

[6] a) B. F. G. Johnson, J. Lewis, B. E. Reichert, K. T. Schorpp, *J. Chem. Soc. Dalton Trans.* **1976**, 1403; b) F. M. Dolgushin, E. V. Grachova, B. T. Heaton, J. A. Iggo, I. O. Koshevoy, I. S. Podkorytov, D. J. Smawfield, S. P. Tunik, R. Whyman, A. I. Yanovskii, *J. Chem. Soc. Dalton Trans.* **1999**, 1609; c) M. J. Stchedroff, S. Aime, R. Gobetto, L. Salassa, E. Nordlander, *Magn. Reson. Chem.* **2002**, *40*, 107.

[7] G. Gervasio, R. Giordano, D. Marabello, E. Sappa, *J. Organomet. Chem.* **1999**, *588*, 83.

[8] a) B. Fontal, M. Reyes, T. Suárez, F. Bellandi, J. C. Díaz, *J. Mol. Catal. A* **1999**, *149*, 75; b) B. Fontal, M. Reyes, T. Suárez, F. Bellandi, N. Ruiz, *J. Mol. Catal. A* **1999**, *149*, 87.

[9] a) R. M. Laine, *J. Mol. Catal.* **1982**, *14*, 137; b) L. M. Bavaro, P. Montangero, J. B. Keister, *J. Am. Chem. Soc.* **1983**, *105*, 4977; c) M. Castiglioni, S. Deabate, R. Giordano, P. J. King, S. A. R. Knox, E. Sappa, *J. Organomet. Chem.* **1998**, *571*, 251; d) G. Süss-Fink, G. Meister, *Adv. Organomet. Chem.* **1993**, *35*, 41.

[10] a) S. Alvarez, P. Briard, J. A. Cabeza, I. del Rio, J. M. Fernandez-Colinas, F. Mulla, L. Ouahab, V. Riera, *Organometallics* **1994**, *13*, 4360; b) M. Castiglioni, R. Giordano, E. Sappa, *J. Organomet. Chem.* **1988**, *342*, 111.

[11] a) T. Hayashi, Z. H. Gu, T. Sakakura, M. Tanaka, M. *J. Organomet. Chem.* **1988**, *352,* 373; b) F. Ragaini, A. Ghitti, S. Cenini, *Organometallics* **1999**, *18*, 4925.

[12] a) D. P. Keeton, S. K. Malik, A. Poë, *J. Chem. Soc. Dalton Trans.* **1977**, 233; b) G. Lavigne, N. Lugan, J. J. Bonnet, *Organometallics* **1982**, *1*, 1040.

[13] G. Süss-Fink, G. Herrmann, *J. Chem. Soc. Chem. Commun.* **1985**, 735.

[14] a) M. Tachikawa, J. R. Shapley, C. G. Pierpont, *J. Am. Chem. Soc.* **1975**, *97*, 7172; b) J. A. Cabeza, J. M. Fernandez-Colinas, A. Llamazares, V. Riega, *Organometallics* **1993**, *12*, 4141.

[15] C. R. Bowers, D. P. Weitekamp, *J. Am. Chem. Soc.* **1987**, *109*, 5541.

[16] a) C. R. Bowers, D. H. Jones, N. D. Kurur, J. A. Labinger, M. G. Pravica, D. P. Weitekamp, *Adv. Magn. Reson.* **1990**, *14*, 269; b) J. Natterer, J. Bargon, *Prog. Nucl. Magn. Reson. Spectrosc.* **1997**, *31*, 293; c) S. B. Duckett, C. J. Sleigh, *Prog. Nucl. Magn. Reson. Spectrosc.* **1999**, *34*, 71.

[17] a) T. C. Eisenschmid, J. McDonald, R. Eisenberg, R. G. Lawler, *J. Am. Chem. Soc.* **1989**, *111*, 7267; b) J. Barkemeyer, M. Haake, J. Bargon, *J. Am. Chem. Soc.* **1995**, *117*, 2927.

[18] a) S. B. Duckett, C. L. Newell, R. Eisenberg, *J. Am. Chem. Soc.* **1993**, *115*, 1156; b) M. Haake, J. Natterer, J. Bargon, *J. Am. Chem. Soc.* **1996**, *118*, 8688.

[19] J. Barkemeyer, J. Bargon, H. Sengstschmid, R. Freeman, *J. Mag. Res. Series A* **1996**, *120*, 129.

[20] H. Sengstschmid, R. Freeman, J. Barkemeyer, J. Bargon, *J. Mag. Res. Series A* **1996**, *120*, 249.

[21] a) S. B. Duckett, G. K. Barlow, M. G. Partridge, B. A. Messerle, *J. Chem. Soc. Dalton. Trans.* **1995**, 3427; b) S. B. Duckett, R. J. Mawby, M. G. Partridge, *J. Chem. Soc. Chem. Commun.* **1996**, 383; c) S. P. Millar, M. Jang, R. J. Lachicotte, R. Eisenberg, *Inorg. Chim. Acta* **1998**, *270*, 363.

[22] B. A. Messerle, C. J. Sleigh, M. G. Partridge, S. B. Duckett, *J. Chem. Soc. Dalton Trans.* **1999**, 1429.

[23] P. J. Carson, C. R. Bowers, D. P. Weitekamp, *J. Am. Chem. Soc.* **2001**, *123*, 11821.

[24] C. Ulrich, J. Bargon, *Prog. Nucl. Magn. Reson. Spectrosc.* **2000**, *38*, 33.

[25] K. Golman, O. Axelsson, H. Johannesson, S. Mansson, C. Olofsson, J. S. Petersson, *Magn. Reson. Med.* **2001**, *46*, 1.

[26] S. Aime, R. Gobetto, D. Canet, *J. Am. Chem. Soc.* **1998**, *120*, 6770.

[27] S. Aime, W. Dastru, R. Gobetto, A. Russo, A. Viale, D. Canet, *J. Phys. Chem. A* **1999**, *103*, 9702.

[28] B. Bergman, E. Rosenberg, R. Gobetto, S. Aime, L. Milone, F. Reineri, *Organometallics* **2002**, *21*, 1508.

[29] R. Gobetto, L. Milone, F. Reineri, L. Salassa, A. Viale, E. Rosenberg, *Organometallics* **2002**, *21*, 1919.

[30] D. Blazina, S. B. Duckett, P. J. Dyson, B. F. G. Johnson, J. A. B. Lohman, C. J. Sleigh, *J. Am. Chem. Soc.* **2001**, *123*, 9760.

[31] G. Lavigne, N. Lugan, J. J. Bonnet, *Organometallics* **1982**, *1*, 1040.

[32] C. J. Sleigh, S. B. Duckett, R. J. Mawby, J. P. Lowe, *Chem. Commun.* **1999**, 1223.

[33] D. Blazina, S. B. Duckett, P. J. Dyson, J. A. B. Lohman, *Angew. Chem. Int. Ed.* **2001**, *40*, 3874.

[34] S. Aime, R. Gobetto, E. Valls, *Inorg. Chim. Acta* **1998**, *275*, 521.

[35] S. Aime, W. Dastru, R. Gobetto, A. Viale, *Organometallics* **1998**, *17*, 3182.

[36] S. Aime, W. Dastru, R. Gobetto, J. Krause, L. Violano, *Inorg. Chim. Acta* **1995**, *235*, 357.

[37] a) B. E. Mann, *J. Chem. Soc. Dalton Trans.* **1997**, 1457; b) B. F. G. Johnson, *J. Chem. Soc. Dalton Trans.* **1997**, 1473.

[38] J. R. Shapley, S. I. Richter, M. Tachikawa, J. B. Keister, *J. Organomet. Chem.* **1975**, *94*, C43.

[39] a) A. J. Deeming, S. Donovan-Mtunzi, S. E. Kabir, *J. Organomet. Chem.* **1985**, *281*, C43; a) A. J. Deeming, S. Donovan-Mtunzi, S. E. Kabir, P. J. Manning, *J. Chem. Soc. Dalton Trans.* **1985**, 1037; c) R. F. Alex, R. K. Pomeroy, *Organometallics* **1987**, *6*, 2437.

[40] a) J. B. Keister, J. R. Shapley, *Inorg. Chem.* **1982**, *21*, 3304; b) S. Aime, D. Osella, L. Milone, E. Rosenberg, E. *J. Organomet. Chem.* **1981**, *213*, 207.

[41] M. I. Bruce, M. J. Liddell, C. A. Hughes, J. M. Patrick, B. W. Skelton, A. H. White, *J. Organomet. Chem.* **1988**, *347*, 181.

[42] a) C. A. Tolman, *Chem. Rev.* **1977**, *77*, 313; b) C. H. Suresh, N. Koga, *Inorg. Chem.* **2002**, *41*, 1573.

[43] G. Süss-Fink, I. Godefroy, V. Ferrand, A. Neels, H. Stoeckli-Evans, *J. Chem. Soc. Dalton Trans.* **1998**, 515.

[44] M. Haake, J. Barkemeyer, J. Bargon, *J. Phys. Chem.* **1995**, *99*, 17539.

[45] V. Ferrand, G. Süss-Fink, A. Neels, H. Stoeckli-Evans, *J. Chem. Soc. Dalton Trans.* **1998**, 3825.

[46] S. A. Colebrooke, S. B. Duckett, J. A. B. Lohman, *Chem. Commun.* **2000**, 685.

[47] A. J. Deeming, S. Hasso, M. Underhill, *J. Chem. Soc. Dalton Trans.* **1975**, 1614.

[48] Z. Dawoodi, M. J. Mays, P. R. Raithby, K. Henrick, W. Clegg, G. Weber, *J. Organomet. Chem.* **1983**, *249*, 149.

[49] a) A. Choplin, B. Besson, L. D'Ornelas, R. Sanchez-Delgado, J. M. Basset, *J. Am. Chem. Soc.* **1988**, *110*, 2783; b) J. A. Cabeza, J. M. Fernandez-Colinas, A. Llamazares, V. Riera, S. Garcia-Granda, J. F. van der Maelen, *Organometallics* **1994**, *13*, 4352; c) J. A. Cabeza, J. M. Fernandez-Colinas, A. Llamazares, *Synlett.* **1995**, 579.

[50] P. G. T. Fogg, W. Gerrard, *Solubility of Gases in Liquids*, Wiley, Chichester (UK), **1991**.

[51] P. Hübler, R. Giernoth, G. Kümmerle, J. Bargon, *J. Am. Chem. Soc.* **1999**, *121*, 5311.

[52] a) H. Adams, N. A. Bailey, G. W. Bentley, B. E. Mann, *J. Chem. Soc. Dalton Trans.* **1989**, 1831; b) H. Adams, C. M. Agustinho, B. E. Mann, S. Smith, *J. Organomet. Chem.* **2000**, *607*, 175.

[53] D. P. Keeton, S. K. Malik, A. Poë, *J. Chem. Soc. Dalton Trans.* **1977**, 233.

[54] a) B. F. G. Johnson, *Inorg. Chim. Acta* **1986**, *115*, L39; b) B. F. G. Johnson, Y. V. Roberts, *Inorg. Chim. Acta* **1993**, *205*, 175.

[55] R. Eisenberg, *Acc. Chem. Res.* **1991**, *24*, 110.

[56] a) D. M. Heinecke, W. J. Oldhem, *Chem. Rev.* **1993**, *93*, 913; b) P. G. Jessop, R. H. Morris, *Coord. Chem. Rev.* **1992**, *121*, 155; c) F. Maseras, A. Lledos, E. Clot, O. Eisenstein, *Chem. Rev.* **2000**, *100*, 601; d) M. Bergamo, T. Beringhelli, G. D'Alfonso, P. Mercandelli, A. Sironi, *J. Am. Chem. Soc.* **2002**, *124*, 5117.

[57] B. F. G. Johnson, Y. V. Roberts, *Polyhedron*, **1993**, *12*, 977.

[58] S. Aime, M. Ferriz, R. Gobetto, E. Valls, *Organometallics* **2000**, *19*, 707.

[59] a) N. E. Leadbeater, J. Lewis, P. R. Raithby, *J. Organomet. Chem.* **1997**, *543*, 251; b) N. E. Leadbeater, C. Jones *Transition Met. Chem.* **2000**, *25*, 99.

[60] a) A. J. Deeming, S. Hasso, *J. Organomet. Chem.* **1975**, *88*, C21; b) A. J. Deeming, S. Hasso, *J. Organomet. Chem.* **1976**, *114*, 313.

[61] a) S. Aime, W. Dastru, R. Gobetto, J. Krause, L. Matas, A. Viale, *Organometallics* **1996**, *15*, 4967; b) S. Aime, W. Dastru, R. Gobetto, F. Reineri, A. Russo, A. Viale, *Organometallics* **2001**, *20*, 2924.

[62] a) J. A. Cabeza, J. M. Fernandez-Colinas, A. Llamazares, V. Riera, *J. Mol. Catal.* **1992**, *71*, L7; b) M. Castiglioni, R. Giordano, E. Sappa, *J. Organomet. Chem.* **1991**, *407*, 377.

[63] R. F. Alex, R. K. Pomeroy, *Organometallics* **1982**, *1*, 453.

[64] P. Kalck, Y. Peres, J. Jenck, *Adv. Organomet. Chem.* **1991**, *32*, 121.

[65] a) S. K. Hasnip, S. B. Duckett, C. J. Sleigh, D. R. Taylor, G. K. Barlow, M. J. Taylor, *Chem. Commun.* **1999**, 1717; b) S. K. Hasnip, S. A. Colebrooke, C. J. Sleigh, S. B. Duckett, D. R. Taylor, G. K. Barlow, M. J. Taylor, *J. Chem. Soc. Dalton Trans.* **2002**, 743.

[66] a) M. I. Bruce, D. C. Kehoe, J. G. Matisons, B. K. Nicholson, H. R. Reiger, M. L. Williams, *J. Chem. Soc. Chem. Commun.* **1982**, 442; b) M. I. Bruce, J. G. Matisons, B. K. Nicholson, *J. Organomet. Chem.* **1983**, *247*, 321.

[67] S. Aime, W. Dastru, R. Gobetto, J. Krause, L. Milone, *Organometallics* **1995**, *14*, 4435.

[68] a) S. B. Duckett, C. L. Newell, R. Eisenberg, *J. Am. Chem. Soc.* **1994**, *116*, 10548; b) K. F. Bonhoeffer, P. Harteck, *Z. Phys. Chem.* **1929**, 113.

[69] W. D. Jones, G. P. Rosini, J. A. Maguire, *Organometallics* **1999**, *18*, 1754.

[70] M. L. H. Green, L. L. Wong, A. Sella, *Organometallics* **1992**, *11*, 2660.